

**Seasonal Variation of Total Column Formaldehyde, Nitrogen Dioxide, and Ozone Over Various Pandora Spectrometer Sites with a Comparison of OMI and Diurnally Varying DSCOVR-EPIC Satellite Data**

Jay Herman<sup>1,2</sup> and Jianping Mao<sup>2,3</sup>

<sup>1</sup>GESTAR II University of Maryland Baltimore County, Baltimore, Maryland USA

1000 Hilltop Cir, Baltimore, MD 21250

<sup>2</sup>NASA Goddard Space Flight Center, 8800 Greenbelt Road, Greenbelt, MD 20771, USA

Correspondence: Jay Herman (herman@umbc.edu)

<sup>3</sup>College of Computer, Mathematical and Natural Sciences, University of Maryland, College Park, MD 20740, USA

## Abstract

Observations of trace gases, O<sub>3</sub>, HCHO, and NO<sub>2</sub>, and their seasonal dependence can be observed using satellite and ground-based data from the Ozone Monitoring Instrument (OMI) satellite and Pandora ground-based instruments. Both operate with spectrometers that have similar characteristics in wavelength range and spectral resolution that enable them to retrieve total column amounts of formaldehyde (TCHCHO), and nitrogen dioxide (TCNO<sub>2</sub>), and total column ozone (TCO). The polar orbiting OMI observes at 13:30 ± 0:25 local time plus an occasional second side-scan point 90 minutes later at mid-latitudes. The ground-based Pandora spectrometer system observes the direct sun all day with a temporal resolution of 2 minutes. At most sites, Pandora data show a strong seasonal dependence for TCO and TCHCHO and less seasonal dependence for TCNO<sub>2</sub>. Use of a low pass filter Lowess(3-months) can reveal the seasonal dependence of TCNO<sub>2</sub> for both OMI and Pandora at mid-latitude sites usually correlated with seasonal heating using natural gas or oil. Compared to Pandora, OMI underestimates the amount of NO<sub>2</sub> air-pollution that occurs during most days, since the OMI TCNO<sub>2</sub> retrieval is around 13:30± 0:25 local time, which tends to occur near the frequent minimum of the daily TCNO<sub>2</sub> time series. Even when Pandora data are restricted to between 13:00 and 14:00 hours local time OMI retrieves less TCNO<sub>2</sub> than Pandora over urban sites because of OMI's large field of view. The seasonal behavior of TCHCHO is mostly caused by the release of HCHO precursors from plant growth and emissions from lakes that peak in the summer as observed by Pandora and OMI. Long-term averages show that OMI TCHCHO usually has the same seasonal dependence but differs in magnitude from the amount measured by Pandora and is frequently larger. Comparisons of OMI total column NO<sub>2</sub> and HCHO with Pandora daily time series show both agreement and disagreement at various sites and days with Pandora frequently larger. For ozone, daily time dependent comparisons of OMI TCO with those retrieved by Pandora show good agreement in most cases. Additional diurnal comparisons are shown of Pandora TCO with hourly retrievals during a day from EPIC (Earth Polychromatic Imaging Camera) spacecraft instrument orbiting the Earth-Sun Lagrange point L<sub>1</sub>.

## 1.0 Introduction

Formaldehyde, HCHO, is ubiquitous in the atmosphere and as with other VOCs (Volatile Organic Compounds) are derived from natural and anthropogenic sources, such as plants, animals, biomass burning, fossil fuel combustion, and industrial processes (Zhang et al., 2019; Morfopoulos et al., 2021). Formaldehyde is mainly produced from the oxidation of VOCs such as isoprene, methane, and anthropogenic emissions (Wittrock, 2006). Formaldehyde can also be directly emitted from some sources, such as vehicle exhaust, tobacco smoke, building materials, and wood burning affecting pollution levels both indoors and outdoors. The majority of gaseous and atmospheric formaldehyde derives from microbial and plant decomposition (Peng et al., 2022). HCHO concentrations in the first few kilometers of the atmosphere vary depending on the location, time of day, season, and meteorological conditions. Some of the factors that influence total atmospheric column amounts of HCHO are:

- **Solar radiation:** Formaldehyde is photolyzed by solar ultraviolet radiation (Nussbaumer et al., 2021) and broken down into smaller molecules and radicals. The photolysis rate of formaldehyde depends on the solar zenith angle, the cloud cover, and the atmospheric composition. Generally, formaldehyde photolysis is faster in the summer and during midday.
- **Temperature:** The thermal decomposition rate of formaldehyde increases with temperature, which means it is faster in warmer regions and seasons.
- **Humidity:** Formaldehyde reacts with water vapor in the atmosphere, forming formic acid and hydroxyl radicals. The reaction rate of formaldehyde with water vapor depends on the relative

humidity, which varies with the temperature and the precipitation. Generally, formaldehyde reaction with water vapor is faster in humid regions and seasons.

The largest sources of  $\text{NO}_2$  are obtained from fossil fuel burning from various types of automobiles truck emissions and power generation followed by industrial processes and oil and gas production (Van der A, 2008; Stavrou et al. 2020). Additional sources are soils with natural vegetation, oceans, agriculture with the use of nitrogen rich fertilizers, forest fires, and lightning. In populated areas requiring winter heating, anthropogenic sources of lower tropospheric  $\text{NO}_2$  are larger than natural sources. Nitrogen oxides play a major role in atmospheric chemistry and the production and destruction of ozone in both the troposphere and stratosphere. In the boundary layer high concentrations of both HCHO (Kim et al., 2011) and  $\text{NO}_2$  (Faustini et al., 2014) are health hazards for humans.

TCHCHO, TCNO<sub>2</sub> and TCO in the atmosphere are typically measured by satellite and ground-based instruments.

- Satellite: The Ozone Monitoring Instrument (OMI) is a satellite sensor launched in July 2004 that measures HCHO,  $\text{NO}_2$ ,  $\text{O}_3$ , and other atmospheric constituents from space (Levelt et al. 2018). Detailed descriptions of the OMI instrument are given in Levelt et al. (2006) and Dobber et al. (2006). Briefly, OMI is a side scanning spectrometer instrument (270 to 500 nm in steps of 0.5 nm) with a nadir spatial resolution of  $13 \times 24 \text{ km}^2$ . OMI data can be used to monitor their global distribution and long-term trends, and to investigate the role of  $\text{NO}_2$  and HCHO in atmospheric chemistry and air quality (Lamsal et al., 2014; 2015; Boeke et al., 2011). For ozone, DSCOVR (Deep Space Climate Observatory), located at the Earth-Sun gravitational balance Lagrange point  $L_1$ , contains a filter-based instrument EPIC (Earth Polychromatic Imaging Camera) capable of obtaining TCO once per hour (90 minutes in Northern hemisphere winter) simultaneously for the entire sunlit globe as the Earth rotates (Herman et al., 2018) with nadir resolution of  $18 \times 18 \text{ km}^2$ .
- Ground-based Spectrometer: The Pandora spectrometer system forms a worldwide network of over 150 currently working direct-sun observing instruments that match atmospheric observations with known laboratory spectra of HCHO,  $\text{NO}_2$ , and  $\text{O}_3$  to obtain the total vertical column above the Pandora instrument every 2 minutes from multiple co-added spectra. Pandora uses a single-grating spectrometer and a charge-coupled device (CCD)  $2048 \times 64$ -pixel detector to record the direct-sun spectra in the ultraviolet and visible wavelength range, 280 – 525 nm with an oversampled 0.6 nm spectral resolution. The retrieval algorithm is based on a spectral fitting technique to retrieve the slant column densities of  $\text{O}_3$ , HCHO,  $\text{NO}_2$  and other gases, and then convert them to vertical column densities using geometric air mass factors appropriate for direct-sun observations. Pandora spectrometers have been deployed in various field campaigns and locations to monitor the spatial and temporal variability of TCHCHO and TCNO<sub>2</sub> to validate and improve the satellite observations of TCHCHO (Herman et al., 2009, Tzortziou et al., 2015, Spinei et al., 2018).

Previous validation studies of TCNO<sub>2</sub> and TCHCHO have been made with emphasis on the amount of bias between ground-based and satellite retrievals of total column  $\text{NO}_2$  and HCHO (Pinardi et al., 2020; de Smedt et al., 2021) and references therein. Validation studies using Pandora measurements have shown that OMI TCNO<sub>2</sub> retrievals tend to underestimate the degree of  $\text{NO}_2$  pollution, especially in urban areas where the coarse OMI spatial resolution tends to reduce the spatially averaged amount (Celarier et al., 2008; Lamsal et al., 2014; Judd et al., 2019; Zhao et al., 2019). In addition to the different field of view, the agreement between OMI and Pandora depends strongly on determining the OMI effective air mass

factor for a wide variety of observing and solar zenith angles (Lorente et al., 2017), whereas Pandora uses a simple geometric direct sun airmass factor (Herman et al., 2009, Eq 3). Studies of TCHCHO involving Pandora prior to 2020 are probably not valid because of a problem with internal generation of HCHO in the Pandora instrument (Spinei et al., 2021). More recent studies (Wang et al. 2022) obtain a seasonal dependence of surface concentrations similar to the TCHCHO in this study. The largest sources of error in TCHCHO retrievals are the determinations of the air mass factor for satellite observations and the fact that ozone and formaldehyde have overlapping absorption spectra so that a small error in ozone retrieval can affect the formaldehyde results. A comparison of direct-sun Pandora TCHCHO retrievals with Geostationary Environment Monitoring Spectrometer GEMS shows a similar seasonal dependence (Fu et al., 2025).

This study will examine the offsets and seasonal cycles of total column NO<sub>2</sub>, HCHO, and O<sub>3</sub> seen by the Pandora instruments by examining multi-year (2021 – 2024) time series for seasonal and daily behavior at various sites and will compare with observations made from the OMI satellite overpass measurements (based on OMI gridded 0.25° x 0.25° data) for the Pandora sites. Pandora ozone measurements will be additionally compared to hourly data obtained from EPIC. All of the Pandora data used in this study are after the upgrade of the instruments to eliminate internal sources of HCHO (Spinei, et al., 2021). Part of this study (TCNO<sub>2</sub> and TCO) is an extension of Herman et al. (2019) using Pandora data (2012 – 2017) before the internal upgrade. A difference is that Pandora TCO is now compared with hourly TCO retrieved by DSCOVR-EPIC. Table 1 shows a list of 30 Pandora sites used in this study.

Table 1 List of 30 Pandora locations used in this study in order of appearance

	Pandora Number	Pandora location name	Lat (deg)	Long (deg)	Alt(m)
1	Pan 180 Fig.1,2	Bronx, New York USA	40.868	-73.878	31
2	Pan 64 Fig.3	New Haven, Connecticut USA	41.301	-72.903	4
3	Pan 190 Fig.4	Bangkok, Indonesia	13.785	100.540	6
4	Pan 182 Fig.5	Tel Aviv, Israel	32.113	34.806	8
5	Pan 159 Fig. 6	Wakkerstroom, South Africa	-27.349	30.144	18
6	Pan 20 Fig.7	Busan, Korea	50.798	4.358	107
7	Pan 145 Fig.10	Toronto-Scarborough, Canada	43.784	-79.187	14
8	Pan 134 Fig. 12	Bristol, Pa, USA	40.107	-74.882	10
9	Pan 204 Fig. 12	Boulder, Co USA	40.038	-105.242	161
10	Pan 106 Fig.12,A2	Innsbruck, Austria	47.264	11.385	616
11	Pan 117 Fig.12	Rome Italy	41.907	12.5158	75
12	Pan 193 Fig.12	Tsukuba, Japan	36.066	140.124	51
13	Pan 140 Fig.13,A2	Washington, DC USA	38.922	-77.012	6
14	Pan 166 Fig.7,A2	Philadelphia, Pa USA	39.992	-75.081	6
15	Pan 238 Fig.14	Granada	37.164	-3.605	7
16	Pan 240 Fig. 14	Thessaloniki, Greece	40.6336	22.9561	60
17	Pan 66 Fig.15	Huntsville Alabama USA	34.725	-86.646	22
18	Pan 156 Fig.15	Hampton, Virginia USA	37.020	-76.337	19
19	Pan 39 Figs.12,15	Dearborn, Michigan USA	42.307	-83.149	18
20	Pan 101 Fig.A1	Izania, Spain	28.309	-16.499	24
21	Pan 119 Fig.A1,A2	Athens, Greece	37.998	23.775	130
22	Pan 124 Fig.A1	Comodoro Rivadavia	-45.7833	-67.45	46
23	Pan 131 Fig. A1	Palau	7.3420	134.4722	23
24	Pan 135 Fig.A1,A2	CCNY Manhattan NY USA	40.815	-73.951	34
25	Pan 142 Fig.A1	Mexico City, Mexico	19.326	-99.176	2280



26	Pan 146 Fig.A1	Yokosuka, Japan	35.321	139.651	5
27	Pan 147 Fig.A1	Detroit, Mi USA	42.303	-83.107	178
28	Pan 150 Fig.A1,A2	Ulsan, Korea	35.575	129.190	38
29	Pan 154 Fig.A1	Salt Lake City Ut, USA	40.766	-75,081	1455
30	Pan 162 Fig.A1	Brussels, Belgium	50.798	4.358	107

## 2.0 Examples of Seasonal and Daily Variation of HCHO and NO<sub>2</sub>

Worldwide Pandora total column data can be downloaded from the Austrian Pandonia project website <https://data.pandonia-global-network.org/>. Of interest for this study are the Level-2 (L2) time series ASCII files for direct-sun observations. For example, the Bronx New York City files for Pandora instrument 180 for TCNO<sub>2</sub> data are in Pandora180s1\_BronxNY\_L2\_rnvs3p1-8.txt, TCHCHO in Pandora180s1\_BronxNY\_L2\_rfus5p1-8.txt, and TCO data in Pandora180s1\_BronxNY\_L2\_rout2p1-8.txt with the 9 bold characters identifying the file contents. This naming convention applies to all Pandora sites.

The Pandora data are arranged in irregular columns that are identified in the metadata header for each file. In the current version, column 1 contains the GMT date and time for each measurement and column 39 contains measured column density in moles m<sup>-2</sup> (multiply by 6.02214076x10<sup>23</sup>/2.6867 x10<sup>20</sup> = 2241.4638 to convert to DU where 1 DU = 2.6867 x 10<sup>20</sup> molecules m<sup>-2</sup>). Pandora data also contain measurements of water vapor, and SO<sub>2</sub> total column amounts in different files.

The original OMI data has a resolution of 13 x 24 km<sup>2</sup> at the center of the OMI side-to-side scan. The overpass OMI data is based on the latest gridded version with 0.25° x 0.25° pixel resolution (midlatitudes approximately 30 x 30 km<sup>2</sup>). The closest OMI pixel to each Pandora site within 50 km is used for time-matched comparisons. Long time series use all available Pandora data between 07:00 and 17:00 filtered for data quality (values with large RMS errors and with negative values are removed). Diurnal comparisons with OMI on specified days use Pandora minute-by-minute data that are nearly continuous suggesting that Pandora is observing the direct sun under clear-sky conditions. Clouds cause some scatter in consecutive data points.

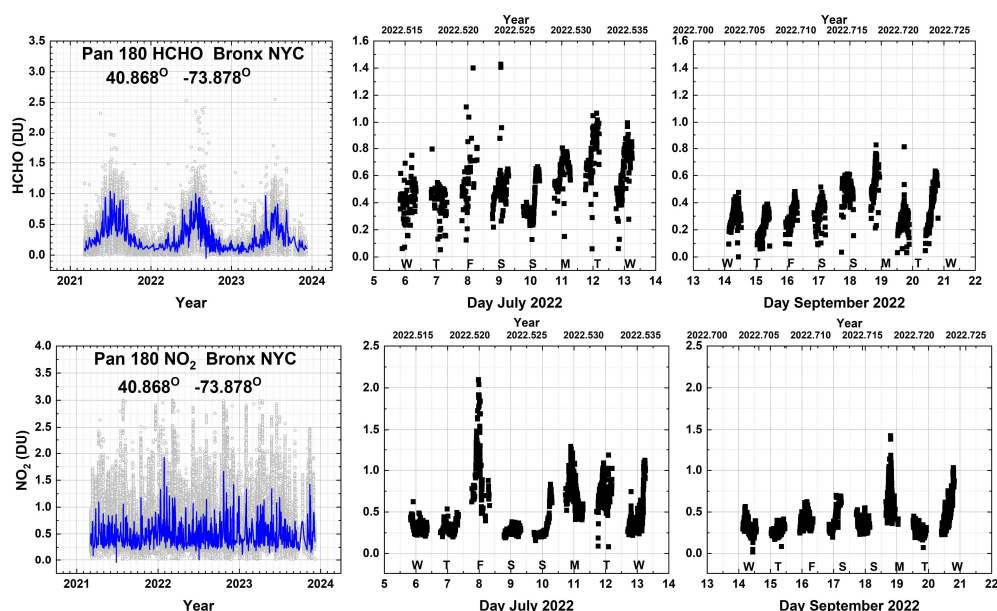


Fig. 01 Seasonal and daily behavior of HCHO and NO<sub>2</sub> from Pan 180 located in the Bronx, NYC at 40.868°N, -73.878°W. The blue lines are a Lowess(0.033) fit to the data (light grey), which is approximately a 1-month local least-squares average. The Local principal investigator for Pan 180 is Dr. Luke Valin.

Figure 1 shows the seasonal and daily variation of total column HCHO (TCHCHO) and NO<sub>2</sub> (TCNO<sub>2</sub>) in Bronx, New York. The daily data for 1 week in July and September shows the range of values for both weekdays and weekends. When all the Bronx TCHCHO data are plotted as an aggregate for 3 years, there is a strong seasonal pattern with a maximum in July and a minimum near the end of December. The summer seasonal dependence of TCHCO is consistent with the surface HCHO values observed by the ground-based Air-Quality System AQS (Wang et al., 2022). For TCNO<sub>2</sub>, there is a weaker seasonal pattern as shown in the Lowess(0.033) fit to the data (Cleveland, 1979; Cleveland and Devlin, 1988) with moderate maxima in January-February, since the sources of NO<sub>2</sub> are largely from the nearly constant flow of cars and trucks. The parameter 0.033 is the fraction of the time-series data included in the local least squares estimate, or about 1 month for Pan 180.

Figure 2 shows the daily average of Pandora data obtained from diurnal variation of TCHCHO and TCNO<sub>2</sub> from 09:00 to 15:00 local standard time (GMT – 5). The primary emission sources of atmospheric HCHO include direct emissions of HCHO precursors from vegetation and lakes, primarily through the release of biogenic volatile organic compounds such as isoprene and terpenes from vegetation, the soil, biomass burning, and decaying plant and animal matter. This is consistent with the Bronx location that is adjacent to a large, vegetated park with a small lake near Fordham University. The same TCHCHO seasonal dependence and magnitude occurs when the Pandora sampling is restricted to 13:00 to 14:00 local standard time similar to the OMI overpass time.

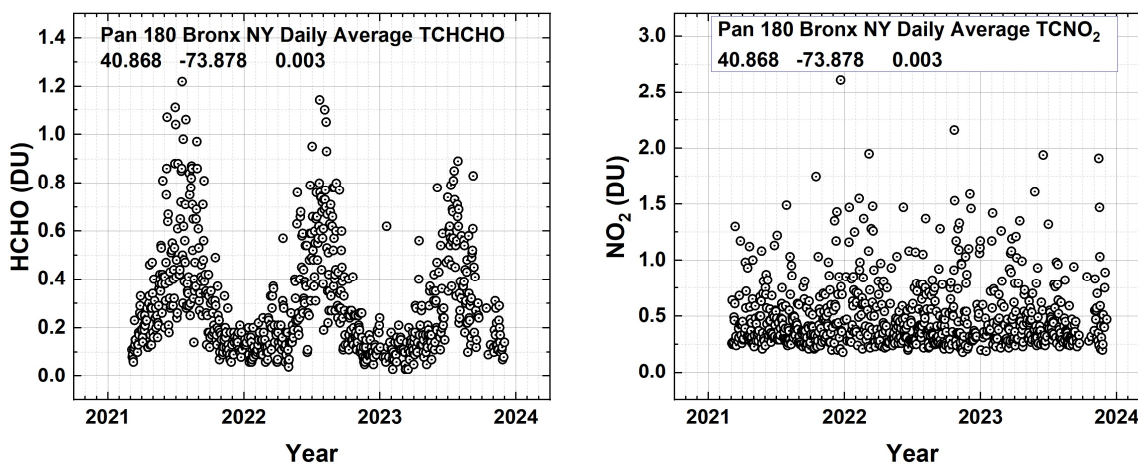


Fig. 02 The daily average seasonal variation of TCHCHO and TCNO<sub>2</sub> in DU over Fordham University in Bronx, New York City from Pandora 180 at 40.868° latitude, -73.878° longitude, and 0.003 km altitude. Each point is a daily average of the data in Fig.1. Local principal investigator: Dr. Luke Valin.

There are 3 Pandora sites in New York City and one in nearby Bayonne, New Jersey. The NYC sites are in the Bronx-Fordham University, Manhattan-City College NY (CCNY), Queens-Queens College. All four successfully measured NO<sub>2</sub> in the period 2021 – 2023. A strong seasonal cycle in TCNO<sub>2</sub> is not seen (Figs. 1 and 2) in the traffic driven production of NO<sub>2</sub> in the Bronx, New York. The mean values of total column

NO<sub>2</sub> (TCNO<sub>2</sub>) for each of the 3 New York sites are 0.5 DU while the TCNO<sub>2</sub> for the port city of Bayonne, NJ is substantially higher at 0.7 DU. None of the four sites show a large seasonal daily average TCNO<sub>2</sub> pattern. For TCHCHO, all four sites show an annual seasonal cycle with three of the sites having a 3-year average of 0.3 DU except for the Queens site at 0.45 DU. The Queens site may be anomalous because of many missing points affecting the average.

Similar behavior is seen at other sites such as the one from New Haven Connecticut located in a vegetated area adjacent to two rivers (Fig.3). TCHCHO has a clear summer peak in June – July and a weak winter TCNO<sub>2</sub> peak in December to January coinciding with the maximum heating season.

The seasonal variation of TCHCHO could not be studied prior to the internal upgrade of Pandora after 2019 that was needed because of the release of HCHO from polyoxymethylene (POM-H Delrin) out-gassing as a function of daytime temperature within the Pandora sun-pointing optical head (Spinei et al., 2021)

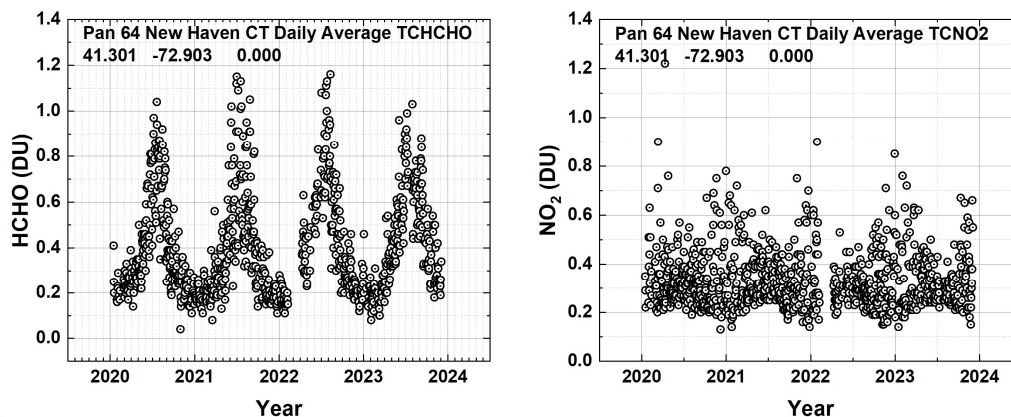


Fig. 03 The seasonal variation of TCHCHO and TCNO<sub>2</sub> over New Haven Connecticut from Pandora 64 at 41.301°N latitude and -72.903°W longitude. Each point is a daily average. Local principal investigator: Dr. Nader Abuhassan

An equatorial Pandora site (Fig. 4) with a sufficiently long data record is located in Bangkok, Indonesia near a small park and lake. Bangkok has a tropical monsoon climate with three main seasons: hot season from March to June, rainy season from July to October, and cool season between November and February. TCHCHO has a seasonal cycle peaking in March – April when the sun is nearly overhead and a minimum during the rainy season. TCNO<sub>2</sub> has a clear seasonal cycle peaking in December – January and a minimum during the rainy season. Bangkok has a tropical climate with April as the hottest month with temperatures averaging at 30.5 °C (87°F) and the coldest is December at 26 °C (79°F).

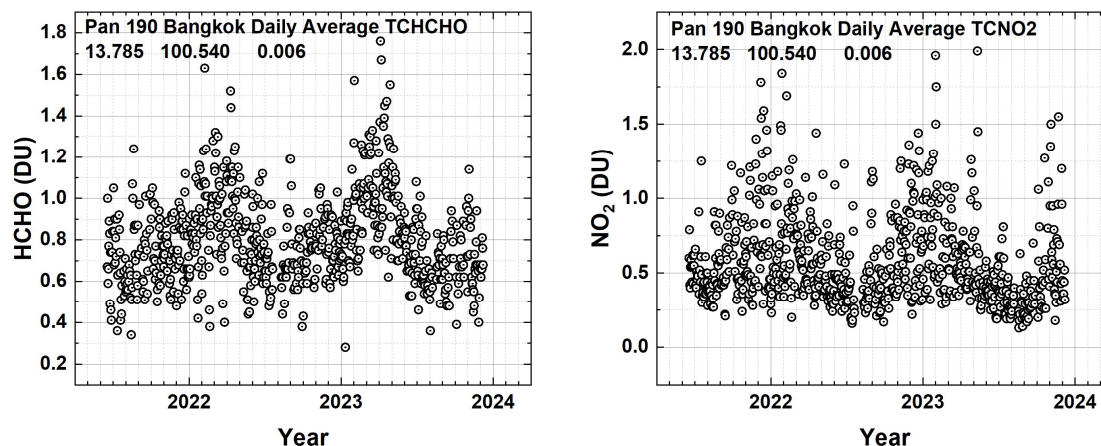


Fig. 04 The seasonal variation of TCHCHO and TCNO2 over equatorial Bangkok Indonesia at  $13.785^{\circ}\text{N}$  and  $100.540^{\circ}\text{E}$ . The local principal investigator is Surassawadee Phoompanit.

209

210 An unusual counter example to the typical TCHCHO seasonal cycle is for the Pandora site located in Tel  
 211 Aviv Israel. Tel Aviv has significant amounts of HCHO but does not show seasonal variation in TCHCHO  
 212 because of a coastal location in a warm climate even at midlatitudes located at  $32.113^{\circ}\text{N}$ ,  $34.085^{\circ}\text{E}$  that  
 213 has essentially two seasons, a cool, rainy winter: October – April and a dry, hot summer: May –  
 214 September. The result is there is a limited seasonal increase in vegetational activity and almost no  
 215 seasonal variation in HCHO (Fig. 5). However, TCNO2 shows a clear seasonal increase in the December -  
 216 January months frequently reaching over 0.5DU. The TCNO2 seasonality is similar to that of the near-  
 217 surface concentrations reported by Boersma et al., (2009). The Pandora instrument 182 is located at Tel  
 218 Aviv University about 1 km from a major highway. Tel Aviv has frequent episodes of smog associated  
 219 with heavy automobile and truck traffic (Newmark, 2001). Heating and cooling in Tel Aviv are mainly  
 220 electrical with the maximum power generation occurring in the summer, suggesting that the winter  
 221 TCNO2 peak is not caused just by electrical power generation from natural gas that emits  $\text{NO}_2$ .

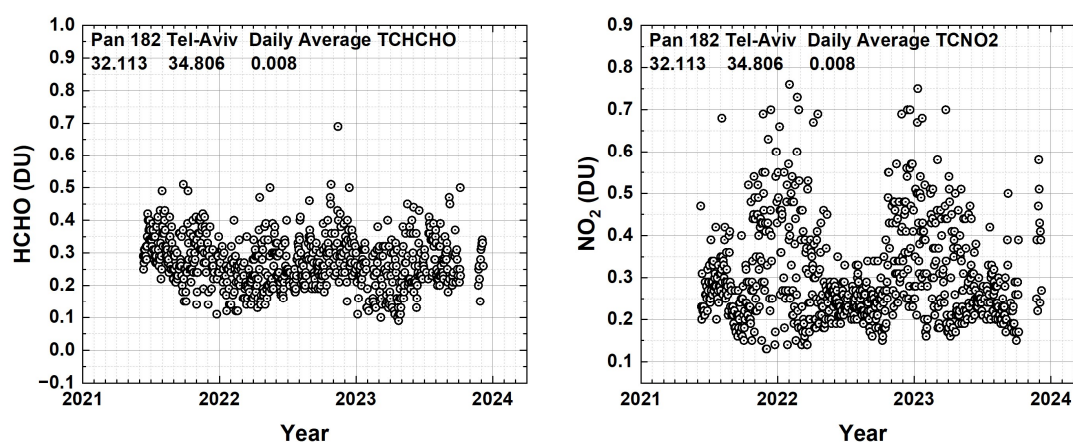


Fig. 05 Seasonal variation in daily average TCHCHO and TCNO2 in Tel Aviv Israel from Pandora 182 located at  $32.113^{\circ}\text{N}$ ,  $34.085^{\circ}\text{E}$  at a height of 8 meters. The local principal investigator for Pan 182 is Dr. Michal Rozenhaimer.

222



223 Finally, a Pandora example from the Southern Hemisphere SH from Wakkerstroom, South Africa located  
 224 in a rural area near the ocean a few degrees outside of the equatorial zone at  $-27.359^{\circ}\text{S}$  and  $30.144^{\circ}\text{E}$ .

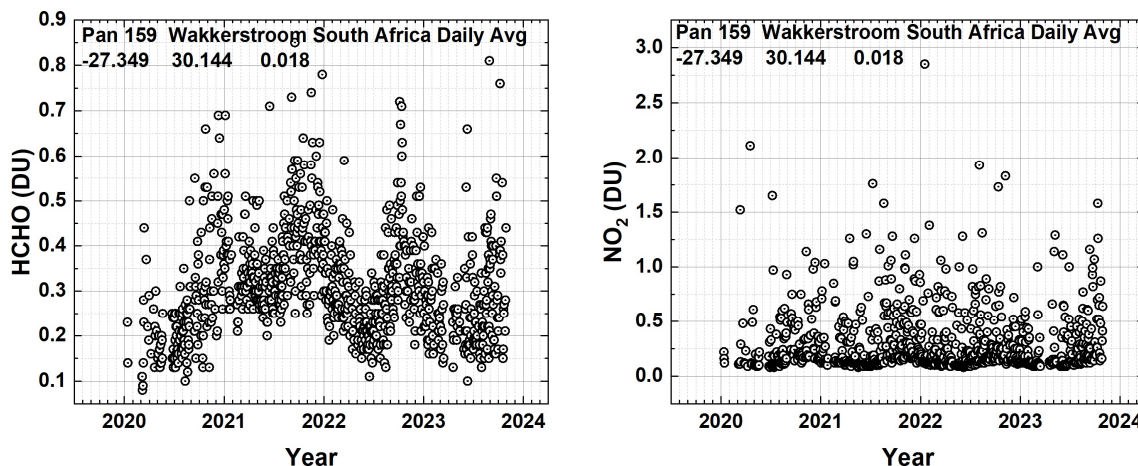


Fig. 06 Seasonal variation in daily average HCHO and  $\text{NO}_2$  in Wakkerstroom South Africa from Pandora 159 located at  $-27.359^{\circ}\text{S}$  and  $30.144^{\circ}\text{E}$  at a height of 18 m. Local principal investigator: B. Scholes

225

226 As expected, the peak value of TCHCHO occurs near the SH summer in November – December, while  
 227 TCNO2 has no significant seasonal dependence.

## 228 2.1 Comparisons Between Pandora and OMI Retrievals of $\text{NO}_2$ and HCHO

229 In this section three types of comparisons of Pandora with OMI satellite data are considered. First (Fig. 7  
 230 upper panels), is the TCNO2 time series consisting of the data record of Pandora and OMI from 2020 –  
 231 2023. The second (Fig. 7 lower panels) is a low-pass Lowess(3-months) filter of midday TCNO2 showing  
 232 the seasonal variation. The third (Fig. 8), looks at a few selected days in May, July, and December and  
 233 compares typical Pandora clear-sky values with the mid-afternoon OMI overpass at times near 13:30  
 234 hours equator crossing time. Pandora and OMI data are matched at the same GMT and then converted  
 235 to local solar time, GMT + Longitude/15. The OMI overpass HCHO,  $\text{NO}_2$  and  $\text{O}_3$  data, 2004 – 2025, are  
 236 found at <https://zenodo.org/uploads/15468213> in 7Zip ASCII format.

237 Figure 7 (upper 2 panels) illustrates that OMI only captures the mid-day fraction of the daily values of  
 238 total column  $\text{NO}_2$  and fails to detect the extent of the daily pollution at both the Bronx New York City  
 239 and Busan Korea sites. This is because OMI and other polar orbiting satellites only collect data once per  
 240 day (occasionally twice per day) at any given location at mid-afternoon, frequently when TCNO2 is  
 241 below its daily maximum (Lamsal et al., 2015; Herman et al., 2019). The lower 4 panels of Fig. 7 reveal  
 242 the seasonal dependence of TCNO2 at two mid-latitude Northern Hemisphere sites found by using a 3-  
 243 month low-pass filter Lowess(3 Months) showing that there is an annual TCNO2 cycle peaking in the  
 244 winter that corresponds to the natural gas and oil heating use. The Pandora (13:00 to 14:00) values are  
 245 larger than those from OMI especially at Busan suggesting that the OMI gridded overpass field of view  
 246  $0.25^{\circ} \times 0.25^{\circ}$  includes areas of lower  $\text{NO}_2$  values over the nearby ocean. In the case of the Bronx, the  
 247 differences are smaller but also include areas over rivers. Philadelphia Pennsylvania is landlocked but  
 248 smaller than an OMI gridded footprint so that the OMI field of view contains somewhat less polluted  
 249 suburbs making the OMI TCNO2 closer to the Pandora values. The Boulder Colorado Pandora is in a

250 small landlocked city where the OMI field of view extends over sparsely populated regions leading to  
 251 OMI TCNO<sub>2</sub> lower than Pandora values.

252

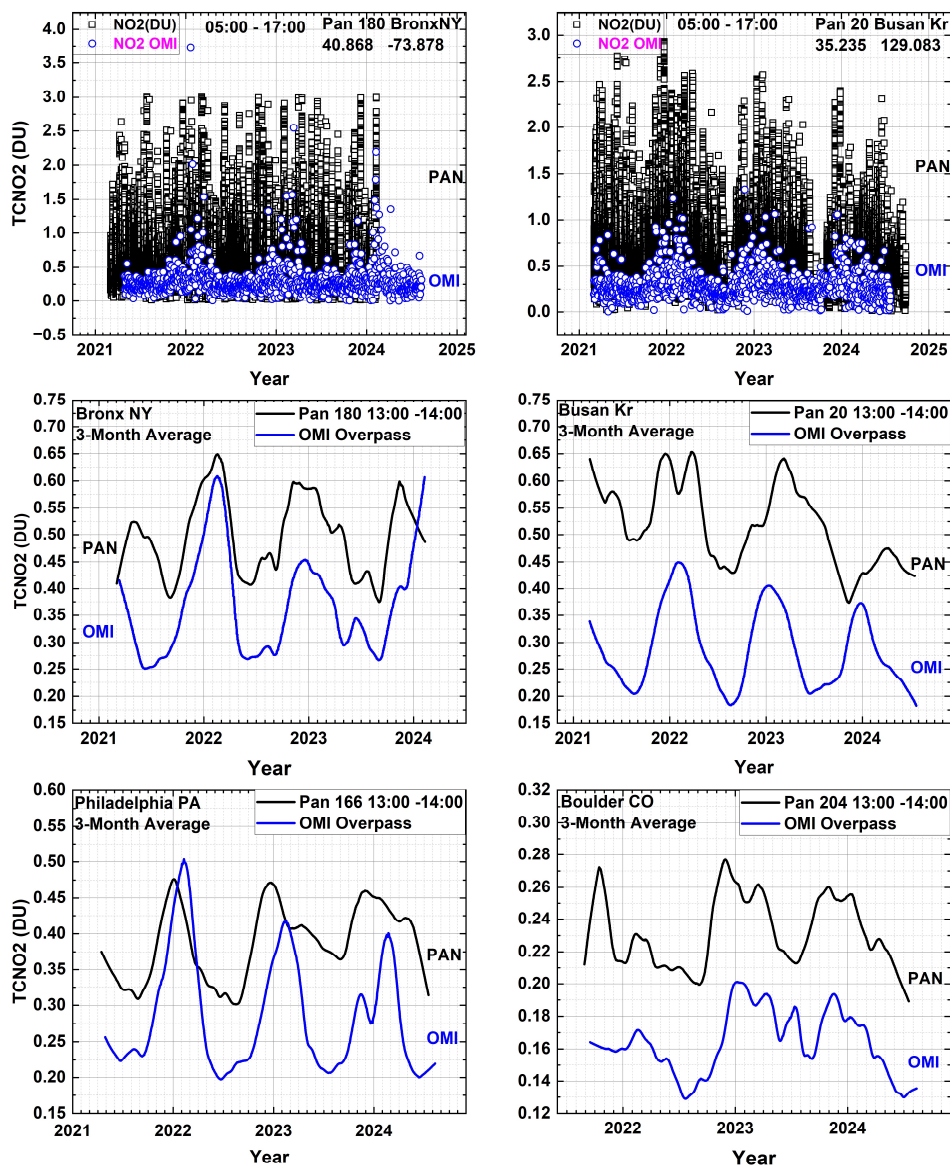


Fig. 07 Upper 2 Panels: Comparison of OMI (approximately 13:30) and Pandora (07:00 – 17:00) total column NO<sub>2</sub> time series in Bronx NY (40.868°N, -73.878°W) and Busan Korea (35.235°N, 129.083°E). Lower 4 Panels: Pandora data for Bronx, Busan, Philadelphia (39.992°N, -75.081°W) and Boulder (40.0375°N, -105.242°W) are averaged between 13:00 – 14:00 hours. Both OMI (blue) and Pandora (black) then have a Lowess(3-month) low-pass filter applied. Local principal investigator for Pan20 is Jae Hwan Kim, for Pan 180 and Pan 166 is Dr. Luke Valin, and for Pan 204 Dr. Nader Abuhassan.

253 Figures 8 and 9 show the diurnal daytime variation for 3 selected days for Pandora retrieved total  
 254 column NO<sub>2</sub> and HCHO compared with OMI at the overpass time for both the Bronx in New York City

255 Busan, Korea and Philadelphia, Pennsylvania. These are typical examples of the highly variable hourly  
 256 variation of TCHCHO and TCNO<sub>2</sub> as observed by Pandora on clear-sky days at most sites.

257

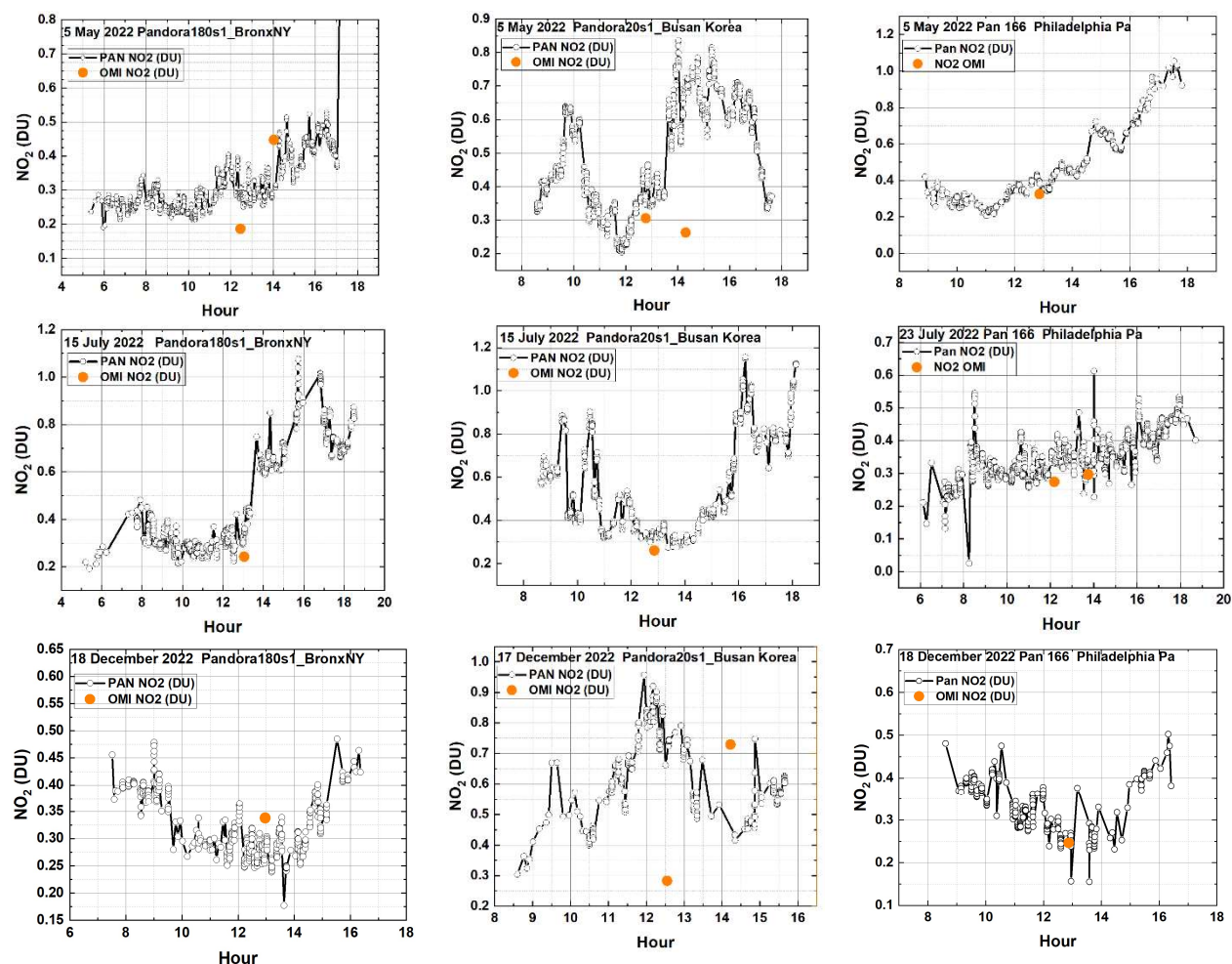


Fig. 08 A comparison between Pandora and OMI (Orange circle) total column NO<sub>2</sub> for 3 locations (Bronx, New York, Busan Korea, Philadelphia, Pennsylvania). The Local principal investigator for Pan 180 and Pan 166 is Dr. Lukas Valin and for Pan 20 is Dr. Jae Hwan Kim.

258

259 The hourly variation of TCHCHO and TCNO<sub>2</sub> on any given day can take on unique shapes depending on  
 260 the presence of surface winds, changes in temperature, and the amount of sunlight. The variability of  
 261 TCNO<sub>2</sub> is also driven by the strength of the sources (automobile exhaust, power generation, industry,  
 262 etc.) as well as the meteorological conditions. On some days, there is good agreement (within 10%) but  
 263 in general the OMI overpass values do not agree with Pandora retrieved values for both TCHCHO and  
 264 TCNO<sub>2</sub>. In the sample shown in Figures 8 and 9, the cases of agreement are about 70% of the time for  
 265 TCNO<sub>2</sub> and 30% for TCHCHO. Also, the OMI TCNO<sub>2</sub> frequently is less than the daily maximum of TCNO<sub>2</sub>.

266

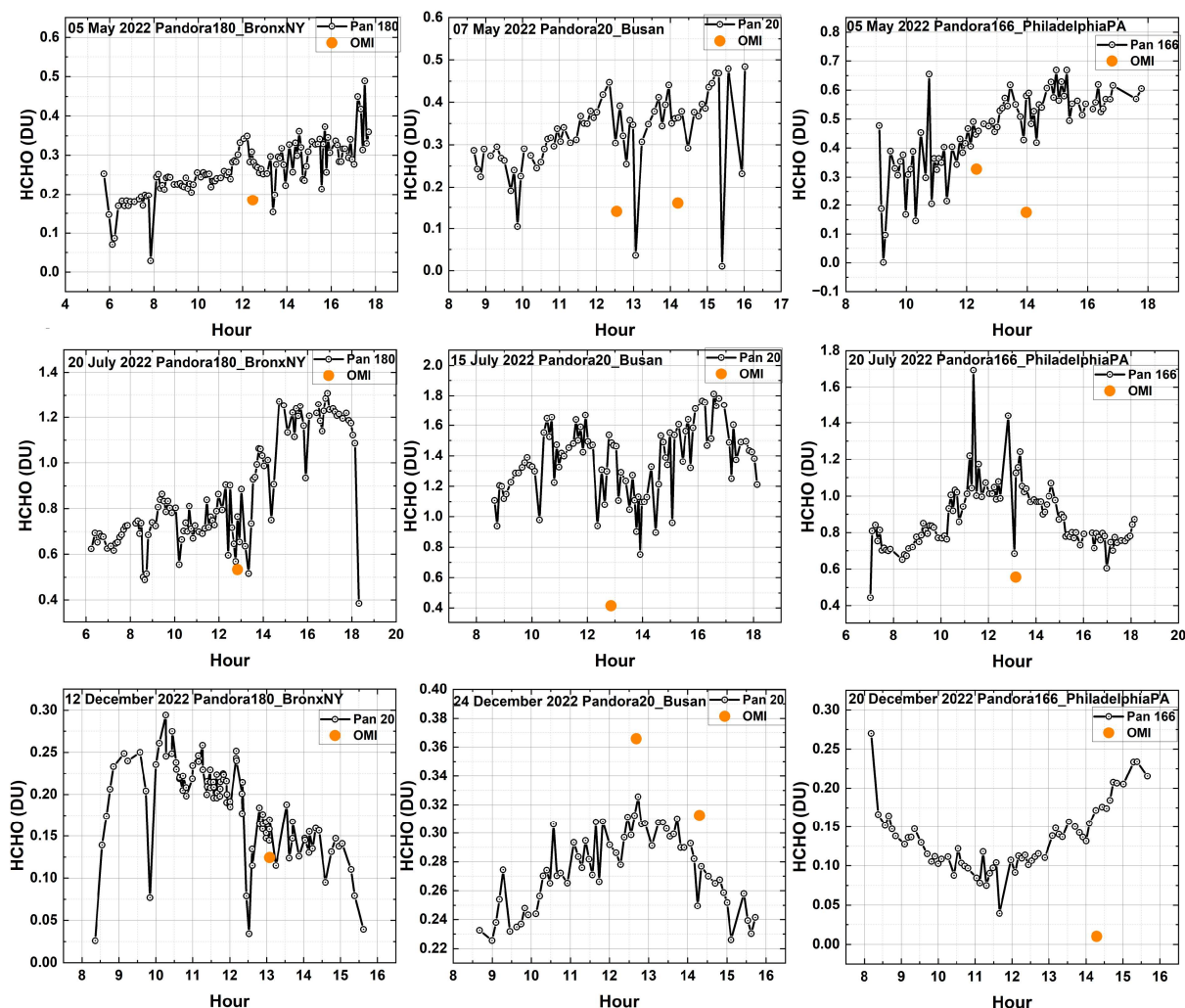


Fig. 09 A comparison between Pandora and OMI (orange circle) total column HCHO. The Local principal investigator for Pan 180 and Pan 166 is Dr. Luke Valin and for Pan 20 is Dr. Jae Hwan Kim.

267

268 Figure 9 illustrates the comparison of TCHCHO retrievals from Pandora and OMI. The spectral fitting  
 269 algorithm for detecting HCHO absorption is in the same short wavelength UV spectral region as used for  
 270 ozone retrieval, 300 – 360 nm (Gratien et al. 2007). This means that the retrieval sensitivity for “seeing”  
 271 all the way to the surface is reduced because of ozone absorption and Rayleigh scattering. Also, small  
 272 errors in ozone retrieval can affect the detection of HCHO. This problem is not present for the spectral  
 273 fitting of NO<sub>2</sub>, since that usually occurs in the visible range 410 – 450 nm where there is only  
 274 interference from a weak and narrow water vapor line.

275 Pandora TCHCHO daily average data (Fig. 10) for University of Toronto in Toronto-Scarborough (Lat =  
 276 43.784°N, Lon = -79.187°W) shows clear peaks in the summer from the vegetation in a surrounding park  
 277 area whereas TCNO<sub>2</sub> shows only small seasonal variation with small peaks also occurring in the summer  
 278 for values less than 0.4 DU. Higher values do not show any seasonal variation. The University of Toronto  
 279 is located near a major highway, which is a strong source of NO<sub>2</sub> from automobiles and trucks. Unlike  
 280 many sites, OMI TCHCHO data over Toronto East (centered on 43.74°N, -79.27°E is about 8 km from the



281 Pandora site) also shows sporadic summer peak values that are higher than the Pandora 13:00-14:00  
 282 averages and all of the Pandora data (Fig. 11).

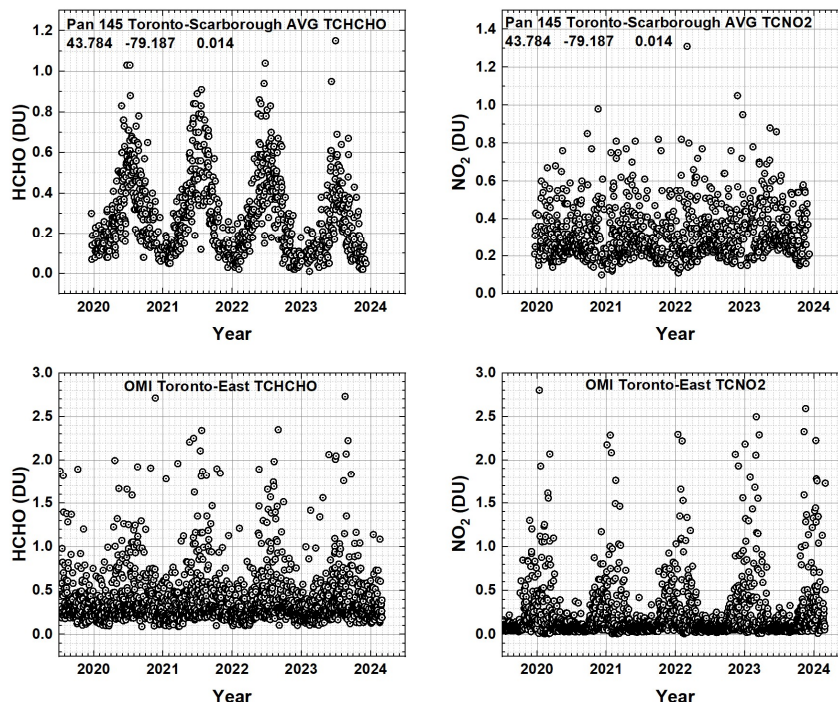


Fig. 10 A comparison of Pandora TCHCHO and TCNO2 daily average total column amounts for Toronto-Scarborough University of Toronto and OMI data for Toronto East (43.740°N, -79.270°W at approximately 13:20±0:20 Local Sun Time, GMT + Longitude/15). The local principal investigator for Pan 145 is Dr. Vitali Fioletov.

283  
 284 Using the daily average Pandora data over Toronto-Scarborough (Fig. 10 upper right) shows no visible  
 285 hint of an TCNO2 annual cycle that peaks in winter while the OMI TCNO2 amounts at 13:40 show a clear  
 286 peak in December – January corresponding to the peak winter heating for the city (Figs. 10 lower right).  
 287 Instead of the daily average data, using the average TCNO2 from 13:00 to 14:00 to correspond to the  
 288 OMI overpass time and then applying a Lowess(3 month) low-pass filter (Fig. 11) shows less TCNO2 and a  
 289 weaker annual cycle that corresponds to the annual cycle observed by OMI. The OMI FOV includes the  
 290 city of Toronto.

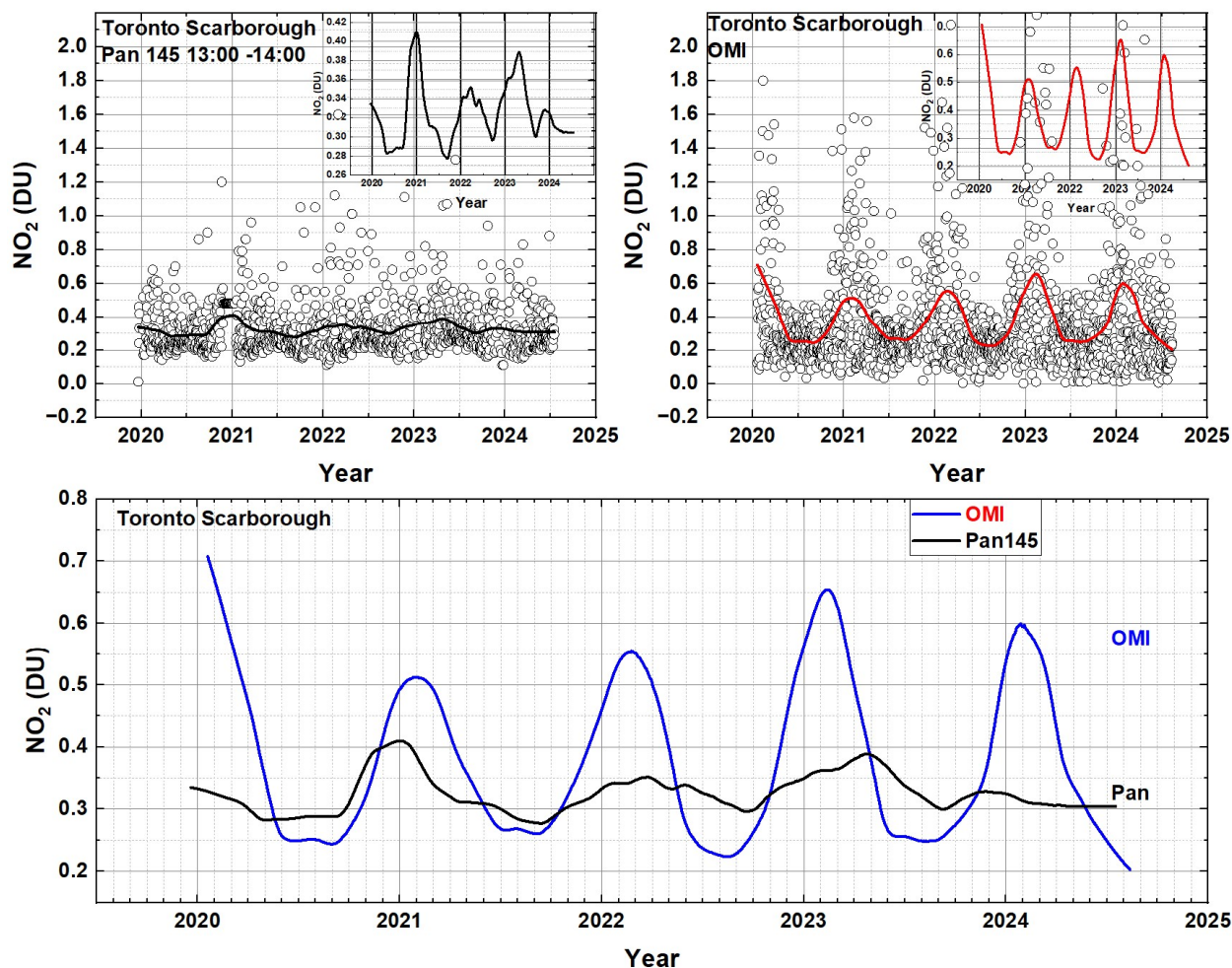


Fig. 11 TCNO<sub>2</sub> annual cycle for Toronto Scarborough from Pan 145 average between 13:00 and 14:00 and OMI. The smooth curves are Lowess(6 Months).

291

292 The lower panel in Fig. 11 reproduces the inset values showing the OMI has a stronger TCNO<sub>2</sub> annual  
 293 cycle because it includes the city area of Toronto. Pandora 145 picks up a small amount of the seasonal  
 294 signal from Toronto.

295 As shown in Fig. 12, the TCHCHO low-pass filtered time series (2021 – 2024), Lowess(3-months),  
 296 measured by OMI and Pandora frequently do not agree. An example is the comparison over Bronx, NY  
 297 (Lat = 40.868° Lon = -73.878°) where the Pandora 180 is located in a park with a small lake, while OMI  
 298 gridded data is averaged over a large area 33 x 33 km<sup>2</sup> in New York City with little vegetation. In 5 of the  
 299 6 sites shown in Fig.12, the OMI retrieval shows more TCHCHO than observed by Pandora. Tsukuba,  
 300 Japan is an exception. Six additional sites are shown in the Appendix Fig. A2.

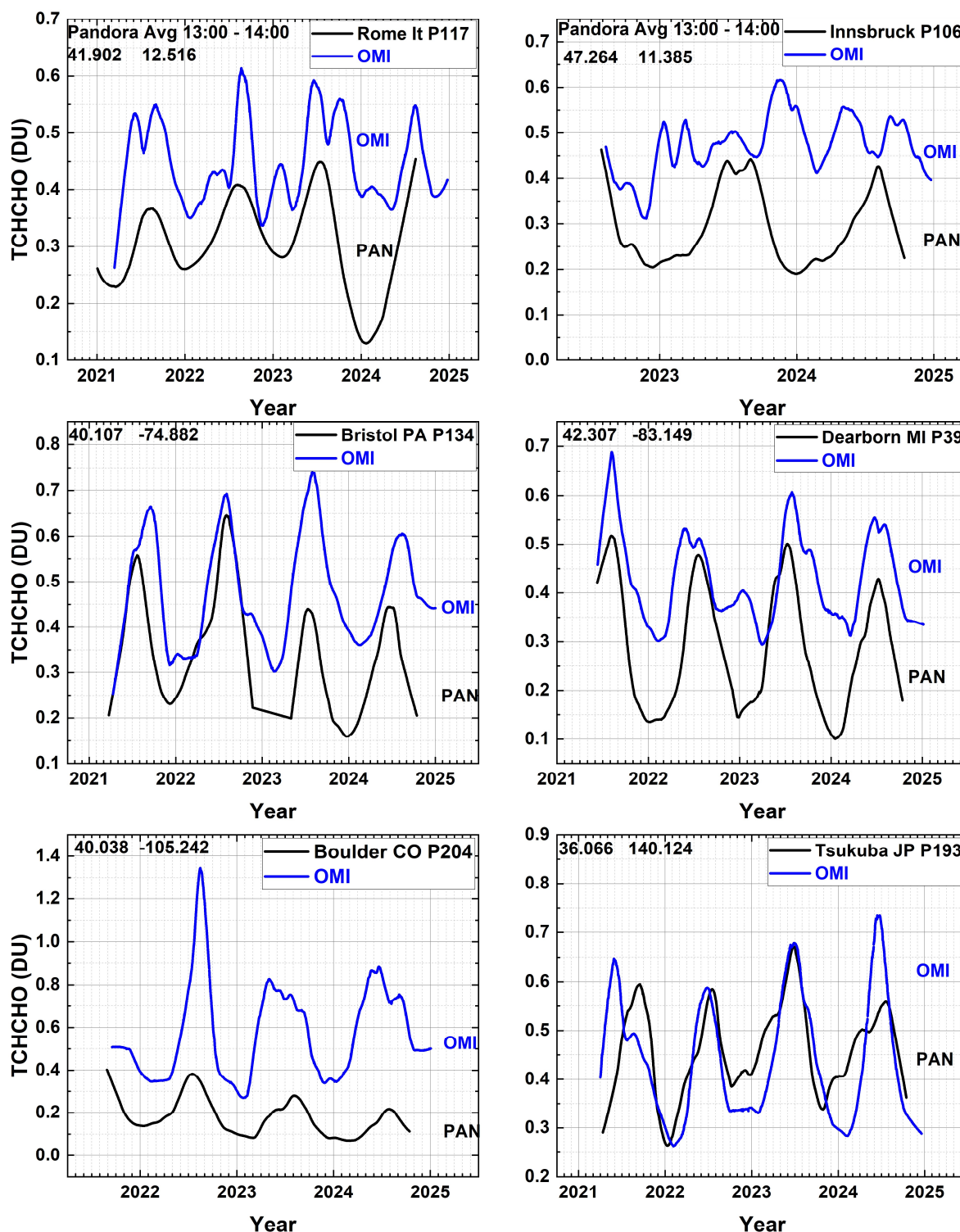


Fig. 12 A comparison between low-pass filtered, Lowess(3 months), OMI and Pandora at six sites with varying degrees of agreement with  $TCHCHO(PAN) < TCHCHO(OMI)$ . The Local Principal Investigators are P106 Dr. Stefano Casadio, Dr. Kei Shiomi P193, Dr. Alexander Cede P204, Dr. Lukas Valin P39; P134, and Dr. Martin Tiefengraber P106. Latitudes and longitudes are in each upper left corner.

The disagreement over Boulder Colorado may be caused by OMI's large field of view that includes lower altitude grasslands. Similarly, the Innsbruck Pandora is located in a valley at the University of Innsbruck surrounded by mountain areas where TCHCHO varies over the OMI FOV. Except for a few cases (e.g., Bronx, NY and Innsbruck, Austria) OMI and Pandora see the same TCHCHO annual cycle.

## 2.2 Total Ozone Column

The retrieval of total column ozone amounts TCO (Figs. 13) serves as a check on the calibration of both OMI and Pandora that is also needed for spectrally overlapping TCHCHO retrievals. Comparisons of Pandora TCO with TCO measured by OMI show good agreement suggesting both instruments are well calibrated in the UV range also needed for retrieving TCHCHO. The good TCO agreement is partly because most of the  $O_3$  is in the stratosphere near 25 km and the fact that ozone is slowly changing spatially over the OMI field of regard for the overpass data. Figure 13 shows an example obtained over Washington DC from the roof of the NASA Headquarters building and from the roof of a building at Pusan University, Korea. The other sites in Table 1 show similar good monthly average agreement.

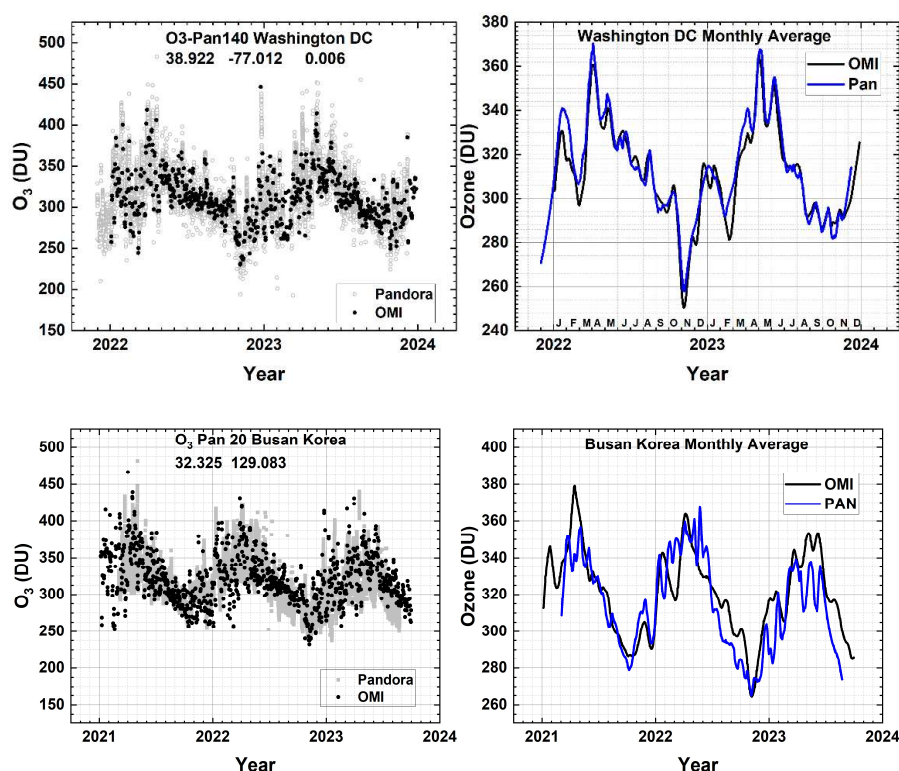


Fig. 13 A comparison of OMI Total Column Ozone values with those obtained from Pandora 140 over the Washington DC site at  $38.922^{\circ}\text{N}$  and  $-77.012^{\circ}\text{W}$  and with those obtained from Pandora 20 over the Busan, Korea site at  $32.325^{\circ}\text{N}$  and  $129.083^{\circ}\text{E}$ . The smooth curves (right panel) are Lowess(6-month) fits to data in the left panel. The local principal investigator for Pan 140 is Dr. Jim Szykman and for Pan20 is Jae Hwan Kim.



318 A test of Pandora UV data is a comparison between EPIC, OMI and Pandora TCO at the specific OMI and  
 319 EPIC overpass times (Fig. 14 and 15). that shows good agreement within 1 to 3 %. OMI TCO overpass  
 320 data for all Pandora sites and more are available from

321 <https://avdc.gsfc.nasa.gov/pub/data/satellite/Aura/OMI/V03/L2OVP/OMTO3/>

322 There is also good agreement between daily OMI TCO with that obtained from Pandora (Fig. 14) at most  
 323 sites. The values obtained at Granada differ by about 8 DU or 2.9 %.

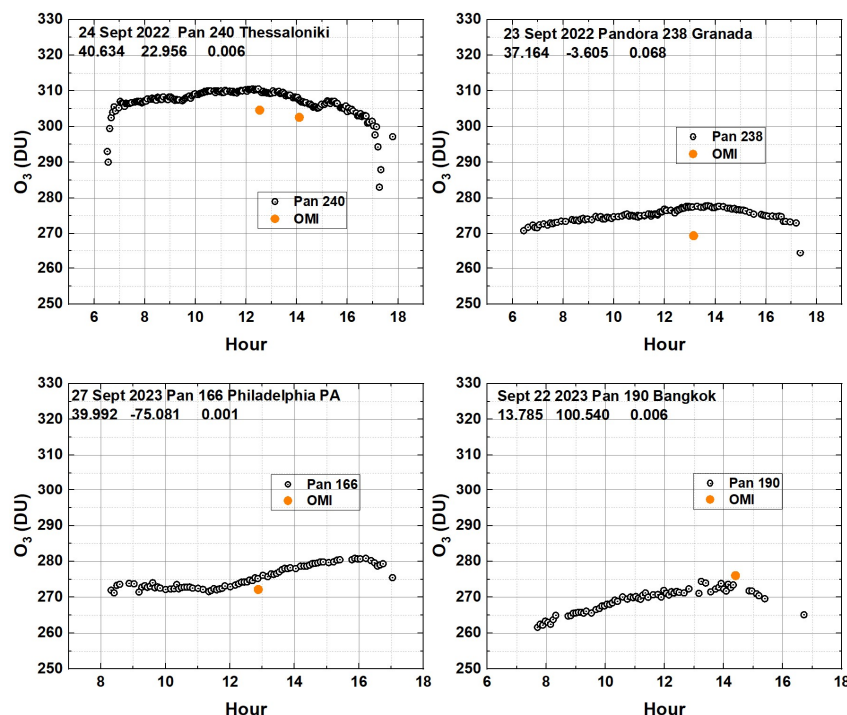


Fig. 14 A comparison of Pandora and OMI retrievals of total column  $O_3$  at the time of the OMI satellite overpass. Local Principal Investigators: Pan 240 Alexander Cede, Pan 238 Inmaculada Foyo Moreno, Pan 166 Lukas Valin, and Pan 190 Surassawadee Phoompan.

The diurnal variation of TCO seen by Pandora can be compared (Fig. 15) with that observed by the Earth Polychromatic Imaging Camera (EPIC) on the DSCOVR (Deep Space Climate Observatory) satellite orbiting about the Earth-Sun gravitational balance Lagrange-1 point (Herman et al., 2018). EPIC obtains simultaneous data from sunrise to sunset once per hour (once per 90 minutes during Northern Hemisphere winter) as the Earth rotates in EPIC's FOV (field of view). Examples of EPIC's view of the whole illuminated Earth are available from <https://epic.gsfc.nasa.gov/>. The spatial resolution for TCO is  $18 \times 18 \text{ km}^2$  at the center of the image (the color images have  $10 \times 10 \text{ km}^2$  resolution). Retrievals earlier than 07:00 and after 17:00 are not reliable for EPIC or Pandora because of high solar zenith angle effects (spherical geometry effects for  $\text{SZA} > 75^\circ$ ) not included in the retrieval algorithms. In the case of EPIC, this is compounded by high View Zenith Angles VZA outside of 07:00 to 17:00 local sun time.

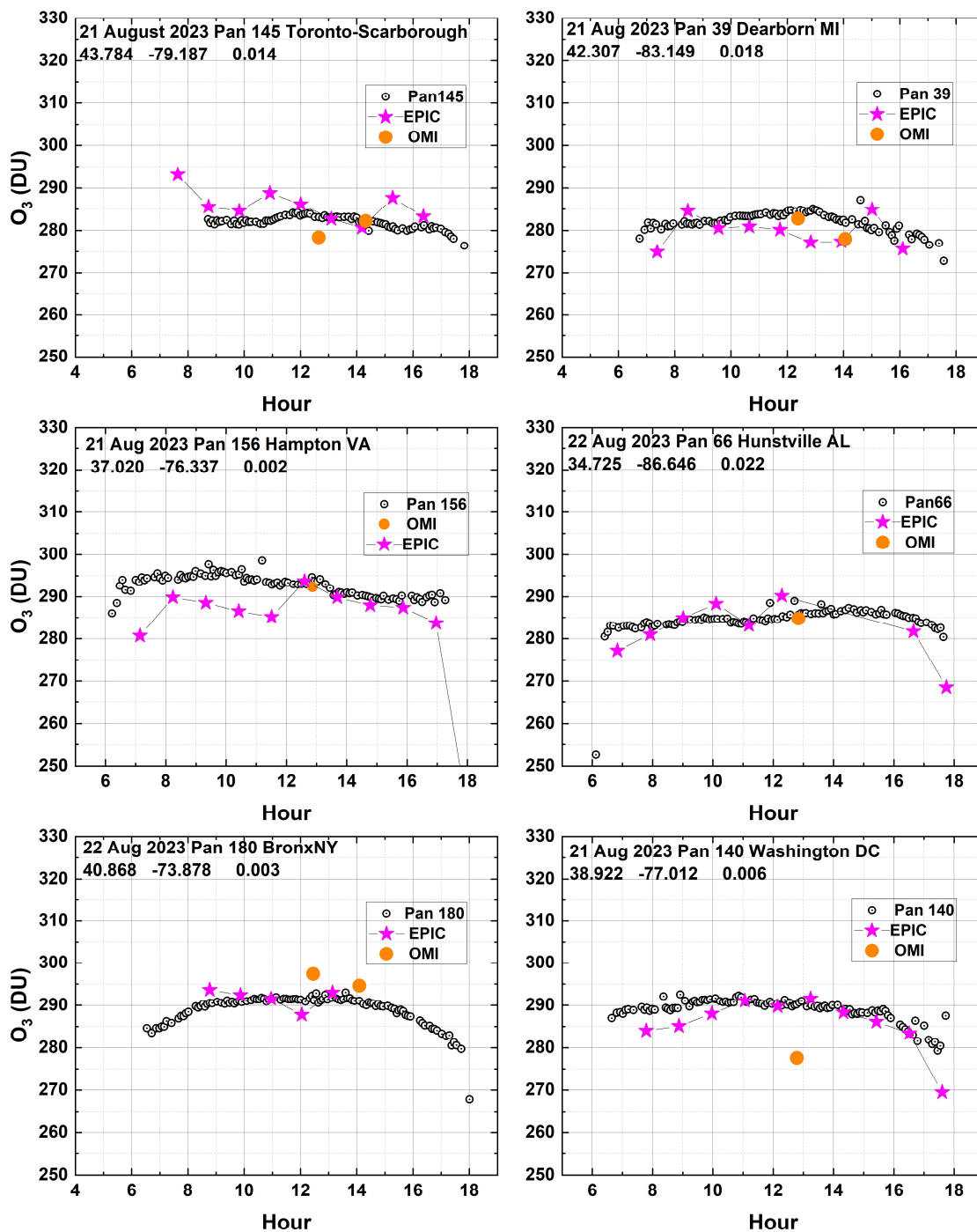


Fig. 15 A comparison of Pandora (Open Circles), EPIC (magenta stars), and OMI (orange circles) retrievals of total column  $O_3$  at the times of the satellite overpasses. Latitude, longitude, and altitude (km) are in the upper left corner. Local Principal Investigators: Pan 145 Vitali Fioletov, Pan 66 Lukas Valin, Pan 39 Lukas Valin, Pan 156 Alexander Cede, Pan 66 Nader Abuhassan, Pan180 Lukas Valin, and Pan 140 Jim Szykman

For the cases shown, the TCO data are properly retrieved between 07:00 and 17:00 local solar time. The 10:20 and 11:30 EPIC value for Hampton, VA of 286.5 and 285DU differs from Pandora by -3 %. Other differences are smaller. Occasionally, OMI differs from Pandora values as is the case, -4.6 %, for 21 August 2023 over Washington, DC.

### 3.0 Summary

Typical examples of the seasonal variability of HCHO, NO<sub>2</sub>, and O<sub>3</sub> in terms of their measured total column TCHCHO, TCNO<sub>2</sub>, and TCO have been presented from both ground-based Pandora Spectrometer instruments and the OMI satellite spectrometer instrument overpass retrievals for selected Pandora sites. For most sites, OMI observes the strong seasonal variation of TCHCHO that is also clearly seen in the Pandora data and in surface measurements (Wang et al., 2022). OMI TCHCHO retrievals are usually larger than those retrieved by Pandora but not always (Fig. A2). The amount of seasonal variation for TCHCHO varies depending on the site. For most midlatitude sites, the seasonal variation is significant with peak values occurring during the summer.

A comparison between the multi-year time series of Pandora and OMI TCNO<sub>2</sub> in urban areas shows that OMI is underestimating the degree of atmospheric NO<sub>2</sub> pollution. The results for TCNO<sub>2</sub> and TCO agree with Pandora data, 2012 – 2017, from a previous study before the Pandora upgrade (Herman et al., 2019). When Pandora is limited to an average of data obtained between 13:00 and 14:00 hours, the agreement between Pandora and OMI TCNO<sub>2</sub> is better but with OMI TCNO<sub>2</sub> frequently less than observed by Pandora. Comparisons of Pandora daily diurnal time series of TCHCHO and TCNO<sub>2</sub> with OMI overpass values show agreement about 30% and 50 % of the time, respectively with OMI frequently retrieving more TCHCHO than Pandora.

OMI TCNO<sub>2</sub> at one shown site, Toronto-Scarborough, shows seasonal variability that the Pandora does not appear to see. However, limiting the data to the OMI overpass time between 13:00 and 14:00 and applying a Lowess(3-months) low-pass filter reveals a weak annual cycle compared to OMI. This could be because OMI detects the NO<sub>2</sub> source from winter heating in the city, while the Pandora site (University of Toronto campus) is fairly remote from Toronto city buildings and is mostly affected by road traffic as the source of NO<sub>2</sub>. The same low-pass filter technique applied to other sites (e.g., Bronx, NY, Busan, Korea, Philadelphia, Pennsylvania, and Boulder, Colorado) also show an annual cycle corresponding to winter heating based on combustion.

Total column ozone agrees well in both seasonal variation and in comparison with Pandora at the OMI overpass time. Given the nature of the ozone retrieval algorithm, the good agreement with TCO suggests that the UV calibrations for the Pandoras and OMI are correct. At most well-calibrated Pandora sites, there is good agreement between Pandora TCO with the hourly TCO obtained from the DSCOVR-EPIC instrument observing the Earth from an orbit about the Earth-Sun gravitational balance Lagrange-1 point.

## 365 Appendix

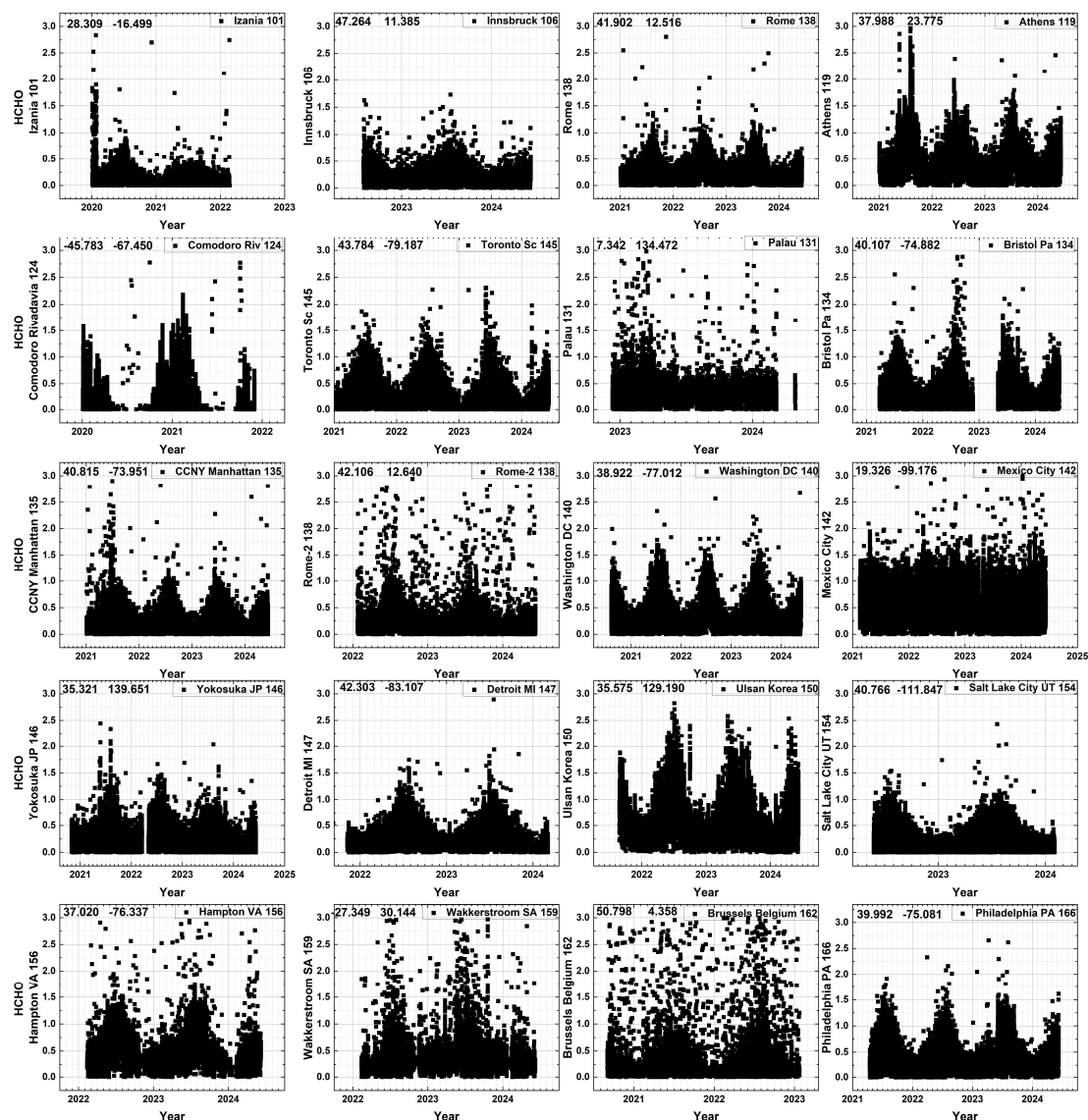


Fig. A1 The seasonal cycle of TCHCHO in DU from 20 randomly selected Pandora TCHCHO time series. The numbers in the upper left corner are the latitude and longitude in degrees and the Pandora instrument number in the right corner.

366

367 Figure A1 shows the seasonal dependence of TCHCHO with the majority of sites showing a maximum  
 368 TCHCHO in mid-summer.



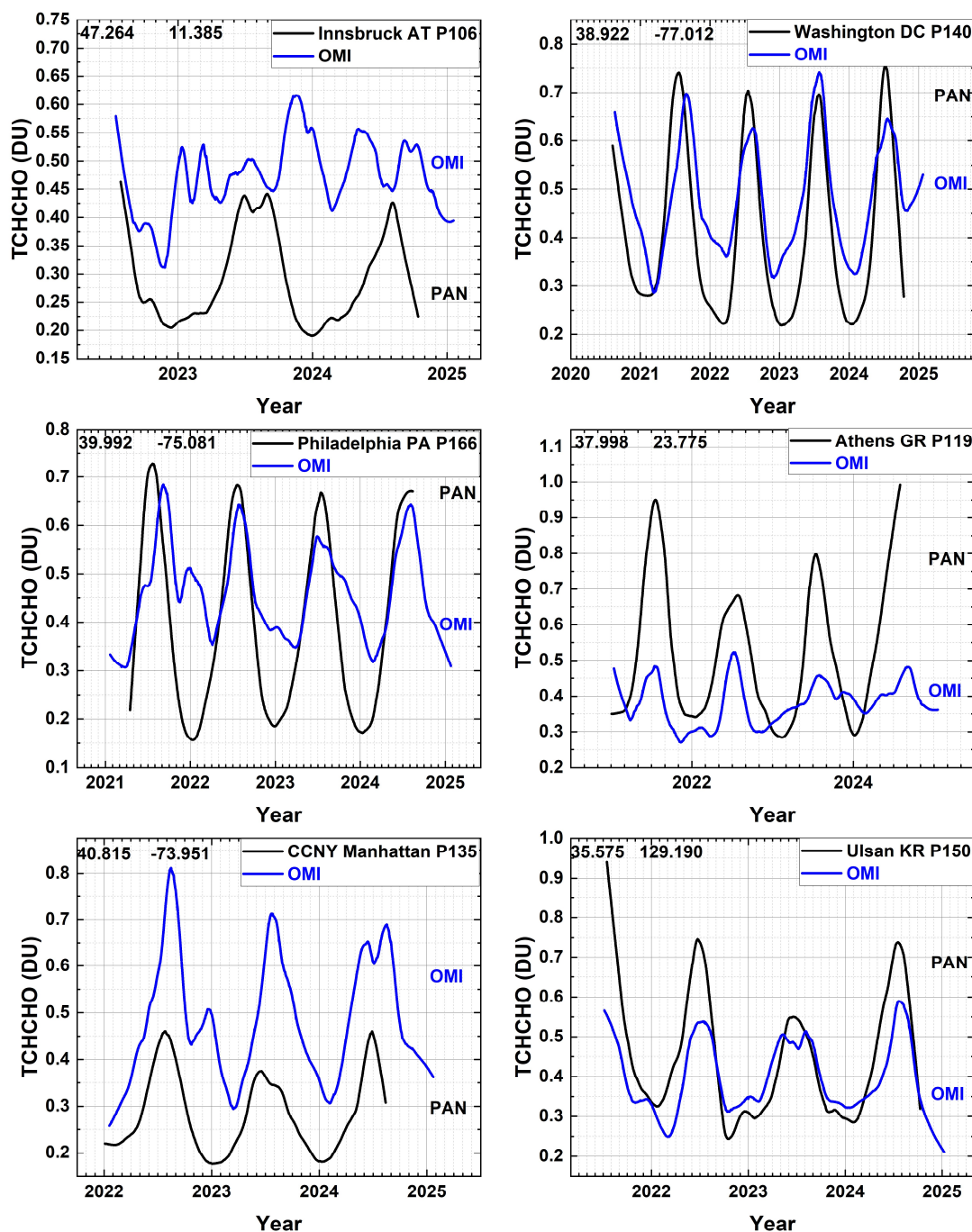


Figure A2 Six cases from Fig. A1 that have significant seasonal variation in TCHCHO. The numbers in the upper left corner are the latitude and longitude in degrees and the Pandora instrument number in the right corner. Principal Investigators are: P106 Dr. Martin Tiefengraber, P140 Dr. Jim Szykman, P166 Dr. Lucas Valin, P119 Dr. Stelios Kazadsi, P135, Dr. Maria Tzortziou, and P150 Dr. Chang Keun Song.

369

370 Figure A2 shows additional cases where OMI and Pandora see the same seasonal dependence but differ  
 371 on the amount of TCHCHO retrieved.

## 4.0 References

- Boeke NL, Marshall JD, Alvarez S, Chance KV, Fried A, Kurosu TP, Rappenglück B, Richter D, Walega J, Weibring P, Millet DB. Formaldehyde columns from the Ozone Monitoring Instrument: Urban versus background levels and evaluation using aircraft data and a global model, *J. Geophys. Res.* 2011 Mar 16;116(D5):10.1029/2010jd014870, doi: 10.1029/2010jd014870, 2011.
- Boersma, Klaas & Jacob, D. & Trainic, Miri & Rudich, Yinon & De Smedt, Isabelle & R, Dirksen & Eskes, Henk, Validation of urban NO<sub>2</sub> concentrations and their diurnal and seasonal variations observed from space (SCIAMACHY and OMI sensors) using in situ measurements in Israeli cities. *Atmos Chem Phys*, 9. 10.5194/acp-9-3867-2009, 2009.
- Celarier, E. A., E. J. Brinksma, J. F. Gleason, J. P. Veefkind, A. Cede, J. R. Herman, D. Ionov, F. Goutail, J.-P. Pommereau, J.-C. Lambert, M. van Roozendael, G. Pinardi, F. Wittrock, A. Schönhardt, A. Richter, O. W. Ibrahim, T. Wagner, B. Bojkov, G. Mount, E. Spinei, C. M. Chen, T. J. Pongetti, S. P. Sander, E. J. Bucsela, M. O. Wenig, D. P. J. Swart, H. Volten, M. Kroon, P. F. Levelt, Validation of Ozone Monitoring Instrument nitrogen dioxide columns, Validation of Ozone Monitoring Instrument nitrogen dioxide columns, *J. Geophys. Res.*, 113,D15S15, doi:10.1029/2007JD008908, 2008.
- Cleveland, W. S.: Robust Locally Weighted Regression and Smoothing Scatterplots, *J. Am. Stat. Assoc.*, 74, 829–836, <https://doi.org/10.2307/2286407> , 1979.
- Cleveland, W. S. and Devlin, S. J.: Locally Weighted Regression: An Approach to Regression Analysis by Local Fitting, *J. Am. Stat. Assoc.*, 83, 596–610, <https://doi.org/10.1080/01621459.1988.10478639> , 1988.
- De Smedt, I., Pinardi, G., Vigouroux, C., Compernelle, S., Bais, A., Benavent, N., Boersma, F., Chan, K.-L., Donner, S., Eichmann, K.-U., Hedelt, P., Hendrick, F., Irie, H., Kumar, V., Lambert, J.-C., Langerock, B., Lerot, C., Liu, C., Loyola, D., Pithers, A., Richter, A., Rivera Cárdenas, C., Romahn, F., Ryan, R. G., Sinha, V., Theys, N., Vlietinck, J., Wagner, T., Wang, T., Yu, H., and Van Roozendael, M.: Comparative assessment of TROPOMI and OMI formaldehyde observations and validation against MAX-DOAS network column measurements, *Atmos. Chem. Phys.*, 21, 12561–12593, <https://doi.org/10.5194/acp-21-12561-2021> , 2021.
- Faustini, Annunziata and Rapp, Regula and Forastiere, Francesco, Nitrogen dioxide and mortality: review and meta-analysis of long-term studies, *European Respiratory Journal*, 44, 744-753, <https://doi.org/10.1183/09031936.00114713> , 2014.
- Fu, W., Zhu, L., Kwon, A., Park, R. J., Lee, G. T., Smedt, I. D., Liu, S., Li, X., Chen, Y., Pu, D., Li, J., Zuo, X., Zhang, P., Li, Y., Yan, Z., Zhang, X., Zhang, J., Wu, X., Shen, H., . . . Yang, X., Evaluating GEMS HCHO Retrievals With TROPOMI Product, Pandora Observations, and GEOS-Chem Simulations. *Earth and Space Science*, 12(1), e2024EA003894. <https://doi.org/10.1029/2024EA003894> , 2025.
- Gratien, A., B. Picquet-Varrault , J. Orphal , E. Perraudin , J.-F. Doussin and J.-M. Flaud , Laboratory intercomparison of the formaldehyde absorption cross sections in the infrared (1660–1820 cm<sup>-1</sup> and ultraviolet (300–360 nm) spectral regions, *J. Geophys. Res.*, **112** , <https://doi.org/10.1029/2006JD007201>, D05305 1-10, 2007.

- Herman, J., A. Cede, E. Spinei, G. Mount, M. Tzortziou, and N. Abuhassan, NO<sub>2</sub> column amounts from ground-based Pandora and MFDOAS spectrometers using the direct-sun DOAS technique: Intercomparisons and application to OMI validation, *J. Geophys. Res.*, 114, D13307, doi:[10.1029/2009JD011848](https://doi.org/10.1029/2009JD011848), 2009.
- Herman, J., Huang, L., McPeters, R., Ziemke, J., Cede, A., and Blank, K.: Synoptic ozone, cloud reflectivity, and erythemal irradiance from sunrise to sunset for the whole earth as viewed by the DSCOVR spacecraft from the earth sun Lagrange 1 orbit, *Atmos. Meas. Tech.*, 11, 177–194, <https://doi.org/10.5194/amt-11-177-2018>, 2018.
- Herman, J., Abuhassan, N., Kim, J., Kim, J., Dubey, M., Raponi, M., and Tzortziou, M.: Underestimation of column NO<sub>2</sub> amounts from the OMI satellite compared to diurnally varying ground-based retrievals from multiple PANDORA spectrometer instruments, *Atmos. Meas. Tech.*, 12, 5593–5612, <https://doi.org/10.5194/amt-12-5593-2019>, 2019.
- Judd, L. M., Al-Saadi, J. A., Janz, S. J., Kowalewski, M. G., Pierce, R. B., Szykman, J. J., Valin, L. C., Swap, R., Cede, A., Mueller, M., Tiefengraber, M., Abuhassan, N., and Williams, D.: Evaluating the impact of spatial resolution on tropospheric NO<sub>2</sub> column comparisons within urban areas using high-resolution airborne data, *Atmos. Meas. Tech.*, 12, 6091–6111, <https://doi.org/10.5194/amt-12-6091-2019>, 2019.
- Kim, K. H., Jahan, S. A., & Lee, J. T., Exposure to Formaldehyde and Its Potential Human Health Hazards. *Journal of Environmental Science and Health, Part C*, 29(4), 277–299. <https://doi.org/10.1080/10590501.2011.629972>, 2011.
- Lamsal, L. N., Krotkov, N. A., Celarier, E. A., Swartz, W. H., Pickering, K. E., Bucsela, E. J., Gleason, J. F., Martin, R. V., Philip, S., Irie, H., Cede, A., Herman, J., Weinheimer, A., Szykman, J. J., and Knepp, T. N.: Evaluation of OMI operational standard NO<sub>2</sub> column retrievals using in situ and surface-based NO<sub>2</sub> observations, *Atmos. Chem. Phys.*, 14, 11587–11609, <https://doi.org/10.5194/acp-14-11587-2014>, 2014.
- Lamsal, L., Duncan, Bryan, Yoshida, Yasuko, Krotkov, Nickolay, Pickering, Kenneth, Streets, David, Lu, Zifeng, U.S. NO<sub>2</sub> trends (2005–2013): EPA Air Quality System (AQS) data versus improved observations from the Ozone Monitoring Instrument (OMI). *Atmospheric Environment*. 110. 10.1016/j.atmosenv.2015.03.055, 2015.
- Levelt, P. F., Joiner, J., Tamminen, J., Veefkind, J. P., Bhartia, P. K., Stein Zweers, D. C., Duncan, B. N., Streets, D. G., Eskes, H., van der A, R., McLinden, C., Fioletov, V., Carn, S., de Laat, J., DeLand, M., Marchenko, S., McPeters, R., Ziemke, J., Fu, D., Liu, X., Pickering, K., Apituley, A., González Abad, G., Arola, A., Boersma, F., Chan Miller, C., Chance, K., de Graaf, M., Hakkarainen, J., Hassinen, S., Ialongo, I., Kleipool, Q., Krotkov, N., Li, C., Lamsal, L., Newman, P., Nowlan, C., Suleiman, R., Tilstra, L. G., Torres, O., Wang, H., and Wargan, K.: The Ozone Monitoring Instrument: overview of 14 years in space, *Atmos. Chem. Phys.*, 18, 5699–5745, <https://doi.org/10.5194/acp-18-5699-2018>, 2018.
- Morfopoulos C, Müller J-F, Stavrakou T, et al. Vegetation responses to climate extremes recorded by remotely sensed atmospheric formaldehyde. *Glob Change Biol.*, 28, 1809–1822. <https://doi.org/10.1111/gcb.15880>, 2021.

- 465 Lorente, A., Folkert Boersma, K., Yu, H., Dörner, S., Hilboll, A., Richter, A., Liu, M., Lamsal, L. N., Barkley,  
466 M., De Smedt, I., Van Roozendaal, M., Wang, Y., Wagner, T., Beirle, S., Lin, J.-T., Krotkov, N., Stammes, P.,  
467 Wang, P., Eskes, H. J., and Krol, M.: Structural uncertainty in air mass factor calculation for NO<sub>2</sub> and HCHO  
468 satellite retrievals, *Atmos. Meas. Tech.*, 10, 759–782, <https://doi.org/10.5194/amt-10-759-2017>, 2017.
- 469  
470 Newmark, G. (2001). Emissions Inventory Analysis of Mobile Source Air Pollution In Tel Aviv, Israel,  
471 *Transportation Research Record*, Vol. 1750, p. 40-48, <https://doi.org/10.3141/1750-0>, 2001.
- 472 Nussbaumer, C. M., Crowley, J. N., Schuladen, J., Williams, J., Hafermann, S., Reiffs, A., Axinte, R.,  
473 Harder, H., Ernest, C., Novelli, A., Sala, K., Martinez, M., Mallik, C., Tomsche, L., Plass-Dülmer, C., Bohn,  
474 B., Lelieveld, J., and Fischer, H.: Measurement report: Photochemical production and loss rates of  
475 formaldehyde and ozone across Europe, *Atmos. Chem. Phys.*, 21, 18413–18432,  
476 <https://doi.org/10.5194/acp-21-18413-2021>, 2021.
- 477 Peng, W.-X., X.-C. Yue, H.-L. Chen, N.L. Ma, Z. Quan, Q. Yu, C. Sonne, A review of plants formaldehyde  
478 metabolism: Implications for hazardous emissions and phytoremediation, *J. Hazard. Mater.* 436 Article  
479 129304, <https://doi.org/10.1016/j.jhazmat.2022.129304>, 2022.
- 480  
481 Pinardi, G., Van Roozendaal, M., Hendrick, F., Theys, N., Abuhassan, N., Bais, A., Boersma, F., Cede, A.,  
482 Chong, J., Donner, S., Drosoglou, T., Dzhola, A., Eskes, H., Frieß, U., Granville, J., Herman, J. R., Holla, R.,  
483 Hovila, J., Irie, H., Kanaya, Y., Karagkiozidis, D., Kouremeti, N., Lambert, J.-C., Ma, J., Peters, E., Piters, A.,  
484 Postlyakov, O., Richter, A., Remmers, J., Takashima, H., Tiefengraber, M., Valks, P., Vlemmix, T., Wagner,  
485 T., and Wittrock, F.: Validation of tropospheric NO<sub>2</sub> column measurements of GOME-2A and OMI using  
486 MAX-DOAS and direct sun network observations, *Atmos. Meas. Tech.*, 13, 6141–6174,  
487 <https://doi.org/10.5194/amt-13-6141-2020>, 2020.
- 488 Spinei, E., Whitehill, A., Fried, A., Tiefengraber, M., Knepp, T. N., Herndon, S., Herman, J. R., Müller, M.,  
489 Abuhassan, N., Cede, A., Richter, D., Walega, J., Crawford, J., Szykman, J., Valin, L., Williams, D. J., Long,  
490 R., Swap, R. J., Lee, Y., Nowak, N., and Poche, B.: The first evaluation of formaldehyde column  
491 observations by improved Pandora spectrometers during the KORUS-AQ field study, *Atmos. Meas. Tech.*,  
492 11, 4943–4961, <https://doi.org/10.5194/amt-11-4943-2018>, 2018.
- 493 Spinei, E., Tiefengraber, M., Müller, M., Gebetsberger, M., Cede, A., Valin, L., Szykman, J., Whitehill, A.,  
494 Kotsakis, A., Santos, F., Abuhassan, N., Zhao, X., Fioletov, V., Lee, S. C., and Swap, R.: Effect of  
495 polyoxymethylene (POM-H Delrin) off-gassing within the Pandora head sensor on direct-sun and multi-  
496 axis formaldehyde column measurements in 2016–2019, *Atmos. Meas. Tech.*, 14, 647–663,  
497 <https://doi.org/10.5194/amt-14-647-2021>, 2021.
- 498 Stavrakou, T., Müller, J.-F., Bauwens, M., Boersma, K. F. & van Geffen, J. Satellite evidence for changes in  
499 the NO<sub>2</sub> weekly cycle over large cities. *Sci. Rep.* <https://doi.org/10.1038/s41598-020-66891-0> (2020).
- 500 Tzortziou, M., Herman, J.R., Cede, A. *et al.* Spatial and temporal variability of ozone and nitrogen dioxide  
501 over a major urban estuarine ecosystem. *J Atmos Chem* **72**, 287–309, [https://doi.org/10.1007/s10874-](https://doi.org/10.1007/s10874-013-9255-8)  
502 [013-9255-8](https://doi.org/10.1007/s10874-013-9255-8), 2015.
- 503 Van der A, R. J., H. J. Eskes, K. F. Boersma, T. P. C. van Noije, M. Van Roozendaal, I. De Smedt, D. H. M. U.  
504 Peters, and E. W. Meijer, Trends, seasonal variability and dominant NO<sub>x</sub> source derived from a ten year  
505 record of NO<sub>2</sub> measured from space, *J. Geophys. Res.*, 113, D04302, doi:10.1029/2007JD009021, 2008.

- 506 Wang, P.; Holloway, T.; Bindl, M.; Harkey, M.; De Smedt, I. Ambient Formaldehyde over the United  
507 States from Ground-Based (AQS) and Satellite (OMI) Observations. *Remote Sens.* 14, 2191,  
508 <https://doi.org/10.3390/rs14092191>, 2022.
- 509 Wittrock, F., Richter, A., Oetjen, H., Burrows, Wittrock, F., Richter, A., Oetjen, H., Burrows, J.P., Kanakidou,  
510 Myriokefalitakis, S., Volkamer, R., Beirle, S., Platt, U., and Wagner, T.: Simultaneous global observations of  
511 glyoxal and formaldehyde from space, *Geophys. Res. Lett.*, 33, L16804,  
512 <https://doi.org/10.1029/2006GL026310>, 2006.
- 513 Zhao, X., Griffin, D., Fioletov, V., McLinden, C., Davies, J., Ogyu, A., Lee, S. C., Lupu, A., Moran, M. D.,  
514 Cede, A., Tiefengraber, M., and Müller, M.: Retrieval of total column and surface NO<sub>2</sub> from Pandora  
515 zenith-sky measurements, *Atmos. Chem. Phys.*, 19, 10619–10642, [https://doi.org/10.5194/acp-19-](https://doi.org/10.5194/acp-19-10619-2019)  
516 [10619-2019](https://doi.org/10.5194/acp-19-10619-2019), 2019.
- 517 Zhang, Y., Li, R., Min, Q., Bo, H., Fu, Y., Wang, Y., & Gao, Z. (2019). The controlling factors of atmospheric  
518 formaldehyde (HCHO) in Amazon as seen from satellite. *Earth and Space Science*, 6, 959–971,  
519 [https://doi.org/ 10.1029/2019EA000627](https://doi.org/10.1029/2019EA000627), 2019.

520 **Author contribution:**

521 Jay Herman is responsible for writing the paper and creating the figures. Jianping Mao obtained the  
522 EPIC overpass data for the Pandora sites and discussed aspects of the paper.

523 **Data Availability**

524 Worldwide Pandora data for 63 sites is available from the Austrian Pandonia project website  
525 <https://data.pandonia-global-network.org/> or from a NASA backup site updated every week.

526 [https://avdc.gsfc.nasa.gov/pub/DSCOVr/Pandora/DATA\\_02/](https://avdc.gsfc.nasa.gov/pub/DSCOVr/Pandora/DATA_02/)

527 The OMI overpass TCHCHO and TCNO2 data are found at

528 <https://avdc.gsfc.nasa.gov/pub/data/satellite/Aura/OMI/V03/L2OVP/OMHCHO/>.

529 <https://avdc.gsfc.nasa.gov/pub/data/satellite/Aura/OMI/V03/L2OVP/OMNO2/>

530 OMI TCO overpass data are available from

531 <https://avdc.gsfc.nasa.gov/pub/data/satellite/Aura/OMI/V03/L2OVP/OMTO3/>

532

533 **Competing interests:**

534 The authors declares that they have no conflicts of interest.

535

536 Funding: This study is funded by the DSCOVr-EPIC project through the University of Maryland  
537 Baltimore County

538

539 **Acknowledgements:**

540 The authors want to acknowledge the contribution of each of the Pandora Principal Investigators  
541 included in the figure captions and for the OMI team and Dr. Lok Lamsal for making OMI overpass  
542 data available. Acknowledgement is also due to the Pandonia team lead by Dr. Alexander Cede for  
543 processing all of the Pandora data and devising the retrieval algorithms and to Dr. Nader Abuhassan  
544 for building and calibrating all of the Pandora spectrometer systems. The Pandonia Global Network  
545 PGN is a bilateral project supported with funding from NASA and ESA.

546

## 547 Figure Captions

548 Fig. 1 Seasonal and daily behavior of HCHO and NO<sub>2</sub> from Pan 180 located in the Bronx, NYC at 40.868°N,  
549 -73.878°W. The blue lines are a Lowess(0.033) fit to the data (light grey), which is approximately a 1-  
550 month local least-squares average. The Local principal investigator for Pan 180 is Dr. Luke Valin.

551 Fig. 2 The daily average seasonal variation of HCHO and NO<sub>2</sub> over Fordham University in Bronx, New  
552 York City from Pandora 180 at 40.868° latitude, -73.878° longitude, and 0.003 km altitude. Each point is  
553 a daily average of the data in Fig.1. Local principal investigator: Dr. Luke Valin

554 Fig. 3 The seasonal variation of TCHCHO and TCNO<sub>2</sub> over New Haven Connecticut from Pandora 64 at  
555 41.301°N latitude and -72.903°W longitude. Each point is a daily average. Local principal investigator:  
556 Dr. Nader Abuhassan.

557 Fig. 4 The seasonal variation of TCHCHO and TCNO<sub>2</sub> over equatorial Bangkok Indonesia at 13.785°N and  
558 100.540°E. The local principal investigator is Surassawadee Phoompanit.

559 Fig. 5 Seasonal variation in daily average TCHCHO and TCNO<sub>2</sub> in Tel Aviv Israel from Pandora 182 located  
560 at 32.113°N 34.085°E at a height of 8 meters. The local principal investigator for Pan 182 is Dr. Michal  
561 Rozenhaimer.

562 Fig. 6 Seasonal variation in daily average HCHO and NO<sub>2</sub> in Wakkerstroom South Africa from Pandora  
563 159 located at -27.359°S and 30.144°E. Local principal investigator: B. Scholes

564 Fig. 7 Upper 2 Panels: Comparison of OMI (approximately 13:30) and Pandora (07:00 – 17:00) total  
565 column NO<sub>2</sub> time series in Bronx NY (40.868°N, -73.878°W) and Busan Korea (35.235°N, 129.083°E).  
566 Lower 4 Panels: Pandora data for Bronx, Busan, Philadelphia (39.992°N, -75.081°W) and Boulder  
567 (40.0375°N, -105.242°W) are averaged between 13:00 – 14:00 hours. Both OMI (blue) and Pandora  
568 (black) then have a Lowess(3-month) low-pass filter applied. Local principal investigator for Pan20 is Jae  
569 Hwan Kim, for Pan 180 and Pan 166 is Dr. Luke Valin, and for Pan 204 Dr. Nader Abuhassan.

570 Fig. 8 A comparison between Pandora and OMI (Orange circle) total column NO<sub>2</sub> for 3 locations (Bronx,  
571 New York, Busan Korea, Philadelphia, Pennsylvania. The Local principal investigator for Pan 180 and Pan  
572 166 is Dr. Lukas Valin and for Pan 20 is Dr. Jae Hwan Kim.

573 Fig. 9 A comparison between Pandora and OMI (purple circle) total column HCHO. The Local principal  
574 investigator for Pan 180 is Dr. Luke Valin and for Pan 20 is Dr. Jae Hwan Kim.

575 Fig. 10 A comparison of Pandora TCHCHO and TCNO<sub>2</sub> daily average total column amounts for Toronto-  
576 Scarborough University of Toronto and OMI data for Toronto East (43.740°N, -79.270°W at  
577 approximately 13:20±0:20 Local Sun Time, GMT + Longitude/15). The local principal investigator for Pan  
578 145 is Dr. Vitali Fioletov.

579 Fig. 11 TCNO<sub>2</sub> annual cycle for Toronto Scarborough from Pan 145 average between 13:00 and 14:00  
580 and OMI. The smooth curves are Lowess(6 Months).

Fig. 12 A comparison between low-pass filtered, Lowess(3 months), OMI and Pandora at six sites with

varying degrees of agreement with  $TCHCHO(Pan) < TCHCHO(OMI)$ . The Local Principal Investigators are P106 Dr. Stefano Casadio, Dr. Kei Shiomi P193, Dr. Alexander Cede P204, Dr. Lukas Valin P39; P134, and Dr. Martin Tiefengraber P106. Latitudes and longitudes are in each upper left corner.

Fig. 13 A comparison of OMI Total Column Ozone values with those obtained from Pandora 140 over the Washington DC site at  $38.922^{\circ}N$  and  $-77.012^{\circ}W$  and with those obtained from Pandora 20 over the Busan, Korea site at  $32.325^{\circ}N$  and  $129.083^{\circ}E$ . The smooth curves (right panel) are Lowess(6-month) fits to data in the left panel. The local principal investigator for Pan 140 is Dr. Jim Szykman and for Pan20 is Jae Hwan Kim.

Fig. 14 A comparison of Pandora and OMI retrievals of total column  $O_3$  at the time of the OMI satellite overpass. Local Principal Investigators: Pan 240 Alexander Cede, Pan 238 Inmaculada Foyo Moreno, Pan 166 Lukas Valin, and Pan 190 Surassawadee Phoompan.

Fig. 15 A comparison of Pandora (Open Circles), EPIC (magenta stars), and OMI (orange circles) retrievals of total column  $O_3$  at the times of the satellite overpasses. Local Principal Investigators: Pan 145 Vitali Fioletov, Pan 66 Lukas Valin, Pan 39 Lukas Valin, Pan 156 Alexander Cede, Pan 66 Nader Abuhassan, Pan180 Lukas Valin, and Pan 140 Jim Szykman.

Fig. A1 The seasonal cycle of TCHCHO in DU from 20 randomly selected Pandora TCHCHO time series. The numbers in the upper left corner are the latitude and longitude in degrees and the Pandora instrument number in the right corner.

Figure A2 shows additional cases where OMI and Pandora see the same seasonal dependence but differ on the amount of TCHCHO retrieved.



**Author contribution:**

Jay Herman is responsible for writing the paper and creating the figures. Jianping Mao obtained the EPIC overpass data for the Pandora sites and discussed aspects of the paper.

**Data Availability**

Worldwide Pandora data for 63 sites is available from the Austrian Pandonia project website <https://data.pandonia-global-network.org/> or from a NASA backup site updated every week.

[https://avdc.gsfc.nasa.gov/pub/DSCOVr/Pandora/DATA\\_02/](https://avdc.gsfc.nasa.gov/pub/DSCOVr/Pandora/DATA_02/)

The OMI overpass TCHCHO and TCNO2 data are found at

<https://avdc.gsfc.nasa.gov/pub/data/satellite/Aura/OMI/V03/L2OVP/OMHCHO/>.

<https://avdc.gsfc.nasa.gov/pub/data/satellite/Aura/OMI/V03/L2OVP/OMNO2/>

OMI TCO overpass data are available from

<https://avdc.gsfc.nasa.gov/pub/data/satellite/Aura/OMI/V03/L2OVP/OMTO3/>

**Competing interests:**

The authors declares that they have no conflicts of interest.

Funding: This study is funded by the DSCOVr-EPIC project through the University Of Maryland Baltimore County

**Acknowledgements:**

The authors want to acknowledge the contribution of each of the Pandora Principal Investigators included in the figure captions and for the OMI team and Dr. Lok Lamsal for making OMI overpass data available. Acknowledgement is also due to the Pandonia team lead by Dr. Alexander Cede for processing all of the Pandora data and devising the retrieval algorithms and to Dr. Nader Abuhassan for building and calibrating all of the Pandora spectrometer systems. The Pandonia Global Network PGN is a bilateral project supported with funding from NASA and ESA.